THE UNDERWATER APPLICATION OF EXOTHERMIC WELDING

Arthur H. Anderssen

THE UNDERWATER APPLICATION OF EXOTHERMIC WELDING

by

ARTHUR H. ANDERSSEN

B.S., Auburn University
(1962)

SUBMITTED IN PARTIAL FULFILLMENT
OF THE REQUIREMENTS FOR THE
DEGREE OF OCEAN ENGINEER
at the
MASSACHUSETTS INSTITUTE OF
TECHNOLOGY
June, 1972

The Underwater Application of Exothermic Welding

by

Arthur H. Anderssen

Submitted to the Department of Ocean
Engineering on May 12, 1972, in partial
fulfillment of the requirements for the
degree of Ocean Engineer.

ABSTRACT

Existing welding processes which have been adapted for underwater use impose serious problems and often produce welds of questionable quality. This thesis presents an investigation of a process previously untested in the underwater environment. The overall objective of the study is the conceptual design of a device which could be used to exothermicly weld a stud, bar, or padeye to underwater structures. The process is commonly called thermit welding.

Several problem areas of both long and short range interest are considered. A theoretical temperature simulation model is developed and verified. The effects of wetness on weld strength and the ability of the thermit process to weld on a "dirty" surface are investigated experimentally. A conceptual design is prepared using experimental results.

By far the most important conclusion arising out of the study is that the thermit process can be applied successfully underwater.

Thesis Supervisor: Koichi Masubuchi
Title: Professor of Naval Architecture

ACKNOWLEDGEMENTS

I would like to extend my sincere thanks to my thesis advisor, Dr. Koichi Masubuchi, for his assistance, comments and support throughout this project. I am also deeply indebted to my wife, Sharon, who has provided the encouragement necessary to complete the study.

TABLE OF CONTENTS

LIST OF FIGURES

DEFINITION OF SYMBOLS USED

Symbol	Definition	Units
C_ℓ	Specific heat of saturated liquid	Btu/lbm-°F
C_{sf}	Constant dependent upon surface fluid combination	
e	2.71828	
g_0	Conversion factor	lbm-ft/lbf-hr^2
g	Gravitational accelleration	ft/hr^2
h_c	Convective heat transfer coefficient	Btu/hr-ft^2-°F
h_{fg}	Latent heat of vaporization	Btu/lbm
J_0, Y_0	Bessel Functions	
k	Thermal conductivity	Btu/hr-ft-°F
L	Length	in or ft
q/A	Heat flux	Btu/hr-ft^2
r	Radius coordinate	in
t	Time	sec or hr
T	Temperature	°F or °R
z	Depth coordinate	in
α	Thermal difusivity	ft/hr
β	Coefficient of expansion	1/°F
θ	Angle	degrees or radians
μ	Dynamic viscosity	lbm/ft-sec
ρ	Density	lbm/ft
σ	Surface tension	lbf/ft

I. INTRODUCTION

A. THE OVERALL PROBLEM AND ITS SETTING:

Man's capability to work in the ocean environment has increased dramatically. This increased capability has created a new need for cutting and joining techniques which can be applied in the underwater environment. Thus, we see an increased amount of goal directed research around the world in underwater cutting and joining techniques. For example, the petroleum industry's offshore wells have created a need for suitable joining procedures. This need has contributed to the development of underwater hyperbaric welding techniques and hardware over the past few years.

However, underwater arc and oxyacetylene welding using a diver, today and for the foreseeable future, appears limited to depths of less than 1000 feet, even employing recent developments in saturated diving. Yet requirements exist and more will soon develop for welding in depths far greater than this. Considering the fact that about 95 percent of the entire ocean floor is deeper than 1000 feet, there is a strong need for developing a capability for welding in the deep sea, particularly for salvage work. One way to perform the welding work is to use a deep submersible, and employ a welding process which can be controled remotely. The use of an exothermic welding process (thermit) may offer a possible solution. It is a relatively simple process requiring no power supplies, and could be remotely

accomplished once the welding device was positioned.

The possible value of such a device has been recognized particularly by U.S. Navy personnel engaged in salvage work. As a result, toward the end of 1970, the Navy granted funds to the Massachusetts Institute of Technology to investigate characteristics of the thermit reaction in the underwater environment and its applicability to the remote-controlled welding of a 50-ton padeye to underwater structures. The results of this research essentially led to the conclusion that the application of exothermic welding processes in the underwater environment deserved further study. This thesis undertakes that study with particular reference to a means of welding a padeye or stud to a deeply submerged object for salvage purposes.

Before stating more specific objectives, however, the reader might find a brief introduction to thermit welding helpful.

B. EXOTHERMIC WELDING:

Although its use is not as universal as arc welding, for example, thermit welding has been used with considerable success in some applications above water. Consequently, a body of knowledge has evolved which must be understood by those attempting to apply the process to a new environment (such as underwater). For this reason, a brief summary of thermit welding processes and major properties of resulting welds is included here.

When metal oxides having low heats of formation are reacted with reducing agents which, when oxidized, have high heats of formation, the reaction is exothermic. The terminology "thermit welding" refers to the group of welding processes which use the superheated metal and slag produced by the above reaction to achieve coalescense with or without the application of pressure. The following are typical thermit reactions:

Reaction	Theoretical Temp. Achieved
$3Fe_3O_4 + 8Al \rightarrow 9Fe + 4Al_2O_3 + 719.3$ Kcal	5590°F/3088°C
$3FeO + 2Al \rightarrow 3Fe + Al_2O_3 + 187.1$ Kcal	4532°F/2500°C
$Fe_2O_3 + 2Al \rightarrow 2Fe + Al_2O_3 + 181.5$ Kcal	5360°F/2960°C
$3CuO + 2Al \rightarrow 3Cu + Al_2O_3 + 275.3$ Kcal	8790°F/4865°C
$3Cu_2O + 2Al \rightarrow 6Cu + Al_2O_3 + 260.3$ Kcal	5680°F/3138°C
$3NiO + 2Al \rightarrow 3Ni + Al_2O_3 + 206.6$ Kcal	5740°F/3171°C
$Cr_2O_3 + 2Al \rightarrow 2Cr + Al_2O_3 + 546.5$ Kcal	5390°F/2977°C

Reaction	Theoretical Temp. Achieved
$3MnO + 2Al \rightarrow 3Mn + Al_2O_3 + 403.0$ Kcal	4400°F/2427°C
$3MnO_2 + 4Al \rightarrow 3Mn + 2Al_2O_3 + 1041.0$ kcal	5020°F/2771°C

The first reaction above is by far the most common, and the major portion of my discussion will refer to it. The temperature required to initiate the reaction is on the order of 2200°F/1205°C. This temperature is generally provided through an ignition powder which, in turn, is ignited by a spark, electric match, etc. Although the theoretical temperature resulting from the reaction is 5590°F/3088°C, radiant heat losses and losses to the reaction vessel reduce this temperature to about 4600°F/2538°C. In practice, other additions and impurities reduce the temperature of the filler weld metal to about 3800°F/2093°C.

There are several methods of employing thermit in joining. The most common is fusion welding where the molten metal produced by the thermit reaction is allowed to flow between the parts to be joined. The thermit is reacted in a crucible and is tapped into a mold after the reaction is complete and slag separation has occurred. A portion of the molten metal is contained between the parts by the mold and a portion allowed to flow into an overflow chamber or riser. Flow through the mold performs two important functions: surface cleaning and preheating. Welds of various sizes and configurations can be accomplished in this manner with a

variety of mold types. Figures 1 through 3 illustrate various hardware for different applications.

Pressure thermit welding refers to the process where the molten metal and slag are used to provide sufficient heat to join the parts themselves without adding material to the weld. In this method, the thermit composition is controlled so that slag with a high freezing point is produced. The thermit is reacted in a separate crucible, configured in such a way that slag is tapped first into a volume surrounding tightly fitted parts. A frozen layer of slag is then formed next to the parts to be joined before the molten metal enters the mold. The heat content of the molten metal and frozen slag brings the temperature of the parts up to forging level, and sufficient pressure is applied to produce a bond.

A third, more recently applied method of using thermit for joining is thermit brazing. As in pressure thermit welding, thermit mixtures are used solely for their heat content. Brazing fluxes and filler metal are positioned so that when the parts to be joined are exothermicly heated, the flux will clean the surfaces and the brazing material will flow between the parts by capillary action.

The properties of thermit welds are affected mainly by thermit composition and cooling rate. Unfortunately, since most research has been performed by companies having a vested interest in the results, little hard data is

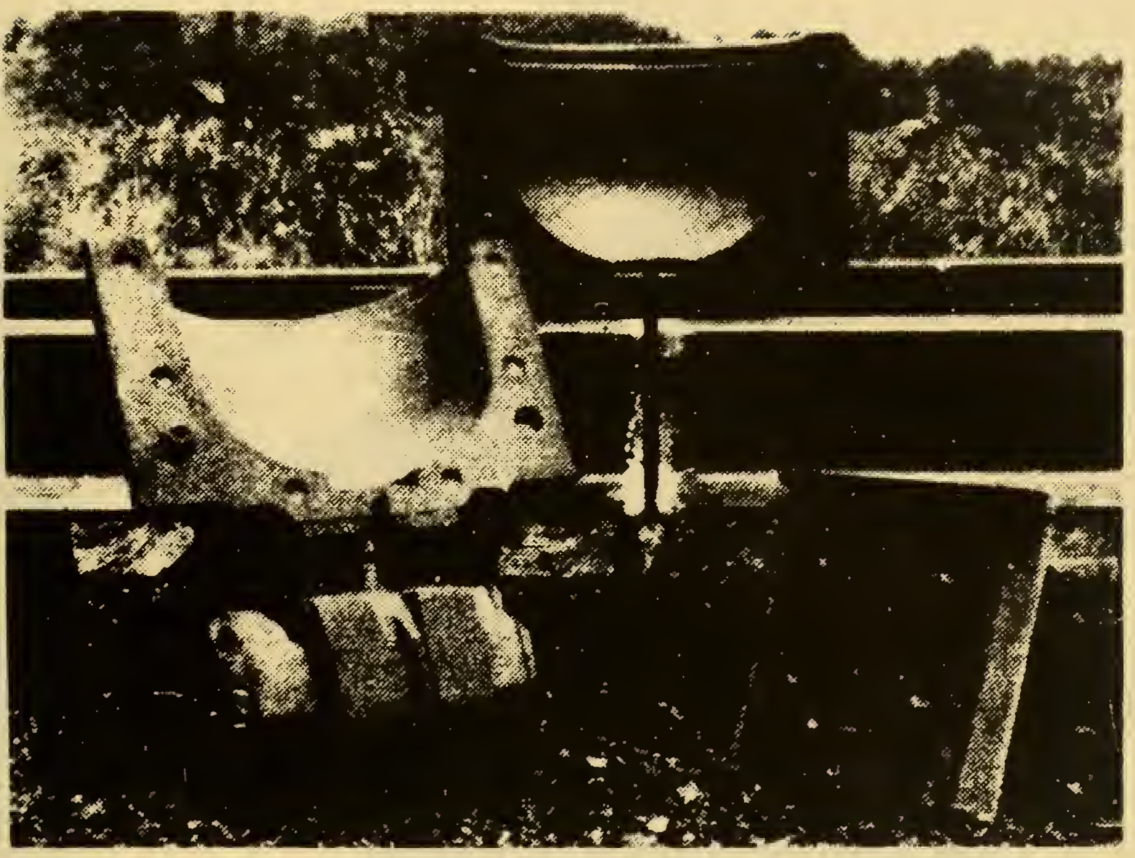

Figure 1: THERMIT WELDING KIT FOR JOINING RAILS

Figure 2: TYPICAL GRAPHITE MOLD FOR JOINING COPPER CABLE

632

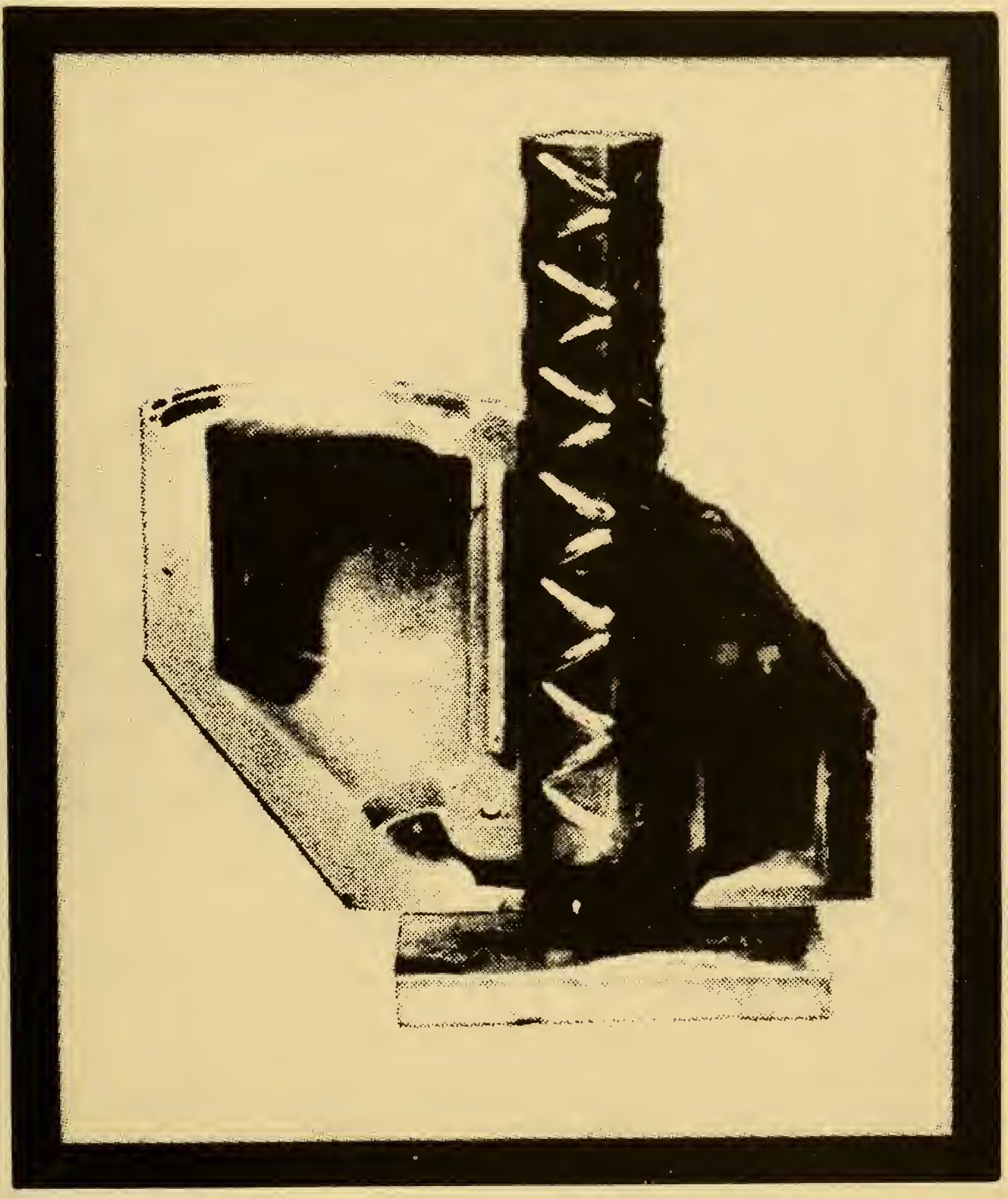

Figure 3: HALF SECTION OF BAR TO PLATE THERMIT WELDING KIT

available. Composition of the weld metal is controlled by adding metallic elements either in the form of pieces or compounds which produce secondary exothermic reactions. The A.W.S. Welding Handbook reports that as cast tensile strengths up to 130,000 psi, and elongations from almost zero to 49 percent are possible by controlling composition. Thermit weld strengths are thus fairly easily matched with the material welded. Figures 4 and 5 illustrate this point through the results of strength tests performed on welded and unwelded reinforcing bars by Thompson and Lichtner Co., Inc.

If the thermit is free of alloying elements (i.e., only Fe_2O_3 and Al are used), the effect of aluminium on weld properties can be determined. As would be expected, excess aluminium serves to reduce porosity, but contributes to brittleness. Silicon has the same effect and is a major cause of brittleness whenever sand molds are used. Manganese also promotes soundness in amounts of about 1 percent and does not have the severe effect on brittleness as do aluminium and silicon.

The cooling rate has a significant influence on resulting hardness. In past research, the exact nature of which is proprietary, hardness of the fusion zone correlated positively with cooling rate. Figure 6 illustrates this effect although exact cooling rate was not determined.

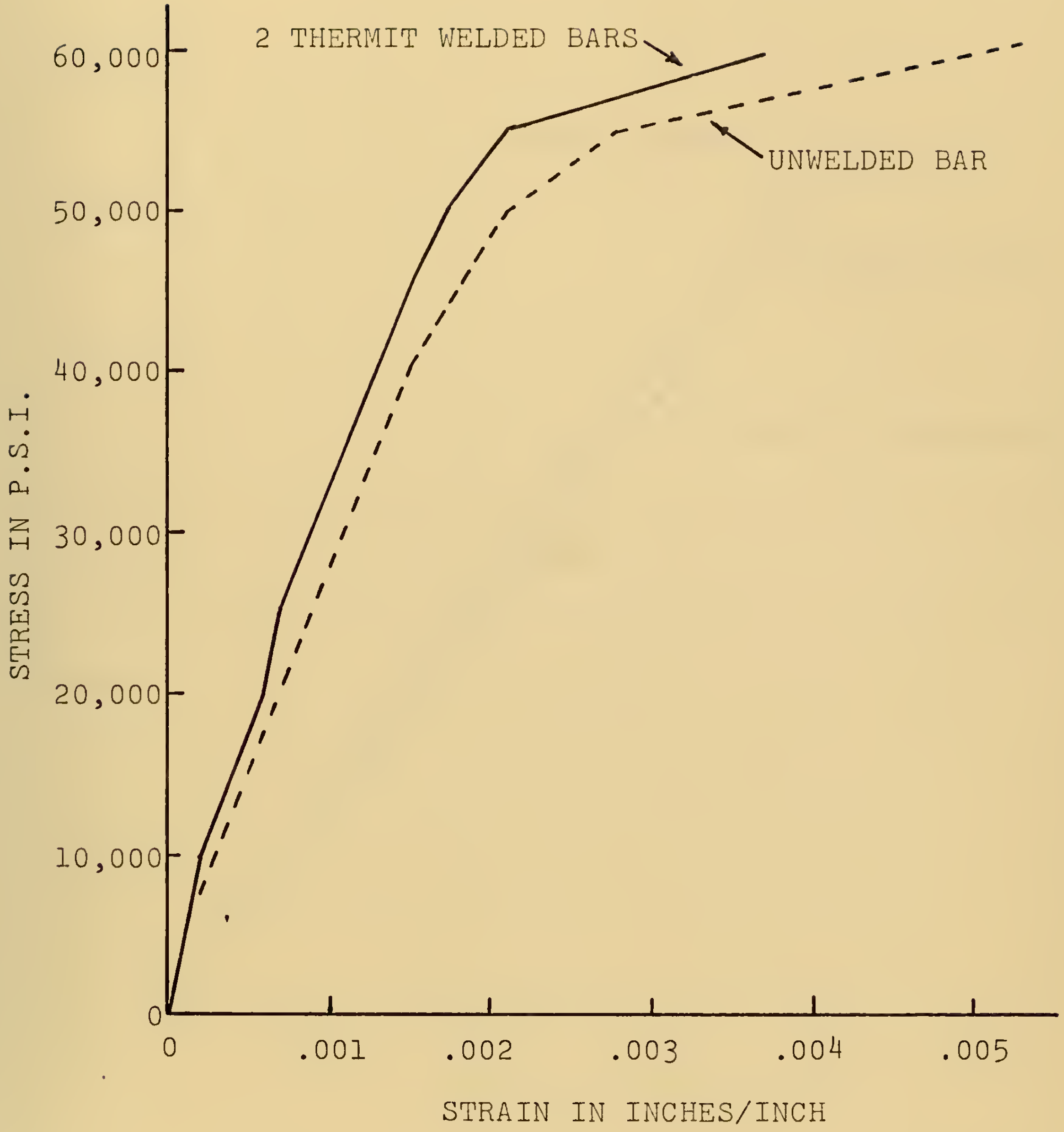

Figure 4: RESULTS OF TENSION TEST ON 18S-INTERMEDIATE GRADE REBARS, SOURCE: THERMEX METALLURGICAL, INC.

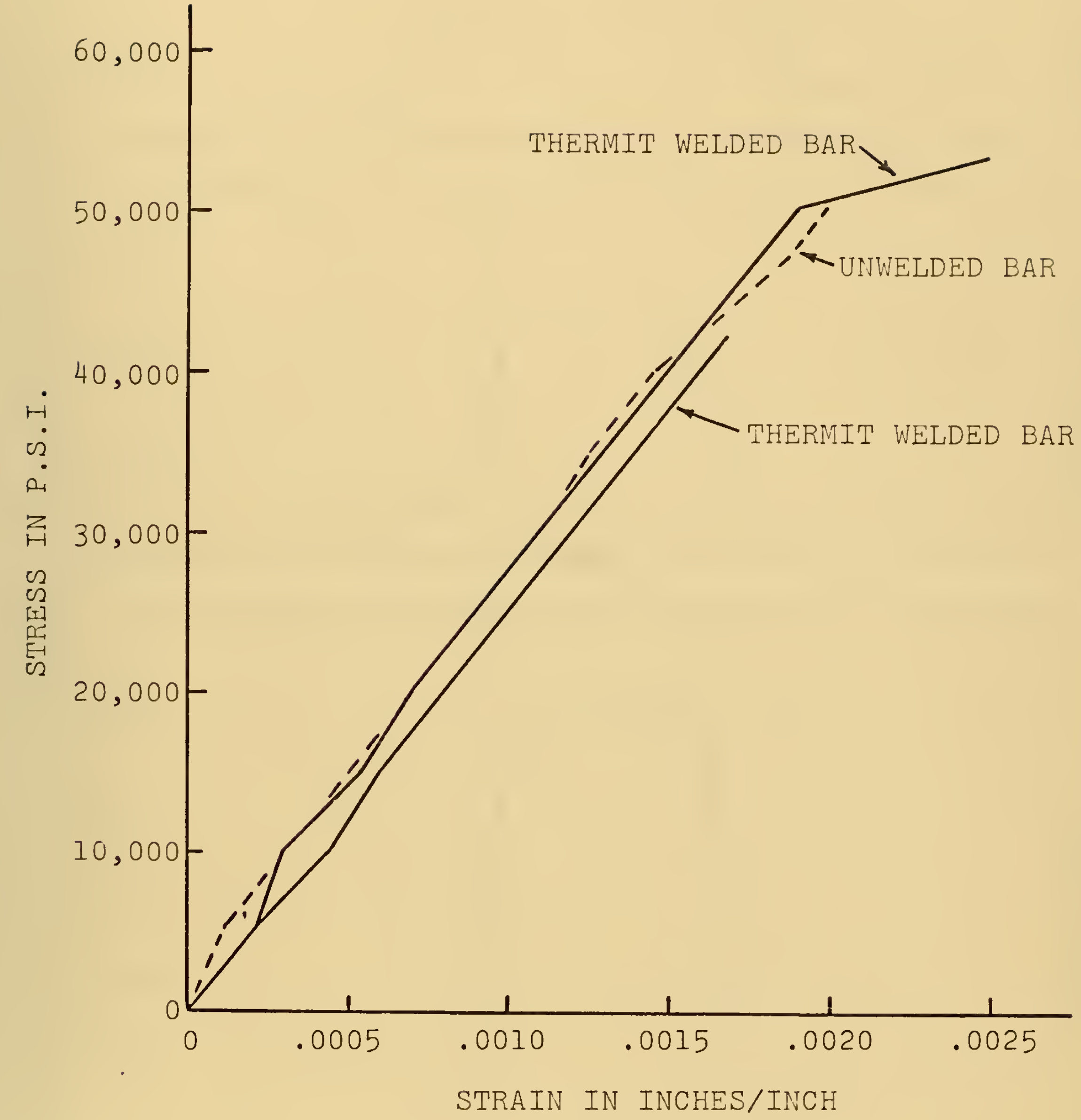

Figure 5: RESULTS OF COMPRESSION TEST ON 18S-INTERMEDIATE GRADE REBARS, SOURCE: THERMEX METALLURGICAL, INC.

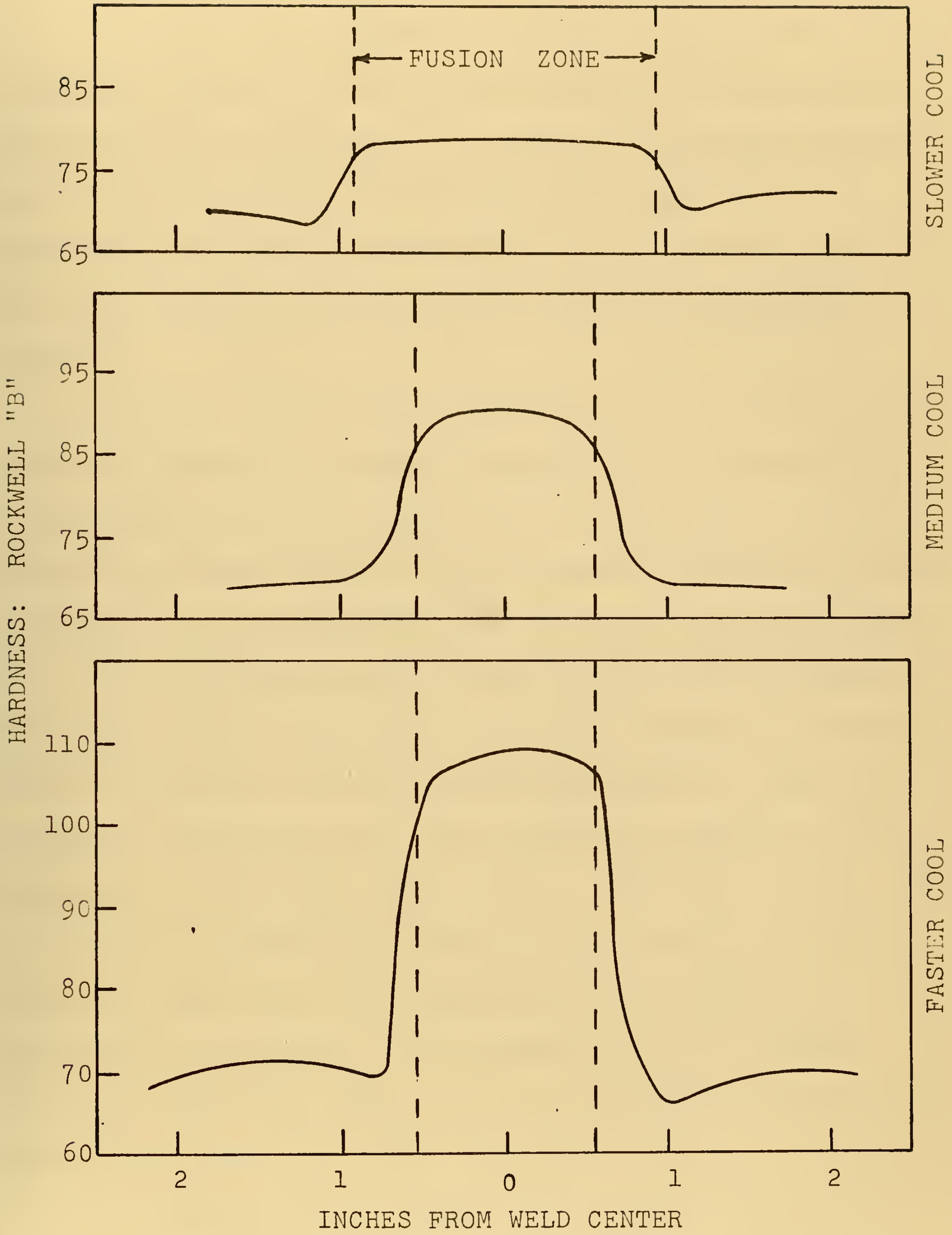

Figure 6: EFFECT OF COOLING RATE ON HARDNESS

C. OBJECTIVES AND APPROACH:

The overall objective of this thesis is the conceptual design of a device which could be used to exothermicly weld a stud, bar, or padeye to underwater structures. As an obstacle to reaching this objective, the underwater environment contributes to five specific problem areas not commonly encountered in above-water exothermic welding.

First, the chemical composition of the environment is vastly different from that encountered on the surface. The presence of water or moisture in the vicinity of the joint to be welded or the reaction chamber, will affect the properties of the weld and the characteristics of the reaction. Wet welds made using other welding processes adapted for underwater use have been shown to be subject to extreme stress corrosion cracking and hydrogen embrittlement as a result of the environment. The objective related to this problem is to determine just how much water or moisture can be tolerated between the surfaces to be welded and still produce a sound weld. The approach to this problem is experimental in nature. It is assumed that the thermit reaction itself must take place in a completely dry environment.

Pressure is a second problem area encountered. Although pressure is one reason that a remotely controllable process such as exothermic welding may be beneficial for

underwater application, device configuration will certainly be influenced by the factor. The objective related to this problem is to determine a means of providing a proper pressure balance between the reaction vessel and the environment at the time of tapping the molten metal. The approach to this problem is analytical in nature.

Surface contamination, although somewhat of a problem above water, is a third problem area underwater. Contamination may vary from minor surface corrosion to painted surfaces to heavy marine growth. Obviously, at the time of welding, the surfaces to be joined must be free of foreign material, implying the need for pre-cleaning by the thermit welding device itself or a separate operation. The objective related to this problem is to determine that degree of surface contamination which can be effectively removed by flow of the molten metal itself between the surfaces to be joined. The approach to this problem is experimental in nature.

A fourth problem area is that of possible water flow velocities in the area where the weld is to be accomplished. Again, device configuration is affected since some means of holding the device in position while welding is accomplished must be devised. However, this problem is believed to be minimal in comparison to the others and is only treated conceptually during the design phase of this study.

Finally, the environment itself forms a large heat sink, affecting cooling rates and ultimately, the properties of the weld. Cooling rates and peak temperatures are of particular interest if thermit welding is found to be a viable process for underwater use, since metallurgical changes and weld properties can be predicted with knowledge of temperature history. Such information might also be useful in design stages if cooling rates could be altered by device configuration. Since the cooling rate problem could have both short and long term impact, a large portion of the thesis is devoted to it. The objective related to this problem area is to develop and verify a model of the thermit bar-to-plate welding process such that the temperature history of the metal could be predicted. The approach is analytical with experimental verification.

D. SUMMARY:

Chapter II covers the development of the temperature simulation model. The exact solution to the heat flow equation is obtained, but since boundary conditions do not permit the evaluation of integration constants, a model using finite difference techniques is constructed.

The experimental procedures are discussed in Chapter III. Data involving temperature histories, wetness level, and cleaning action was obtained during the experiments. Then, theoretical and experimental results are presented and compared in Chapter IV.

Results are utilized in Chapter V to develop a conceptual design of an underwater welding device.

Finally, conclusions and recommendations for further research are presented in Chapter VI.

II. THEORETICAL MODEL FOR HEAT TRANSFER

A. OVERVIEW:

Unlike most welding processes, the heat source in thermit welding has a well defined shape since a mold is used which surrounds the parts to be welded. In addition, the device itself does not move during the welding operation. These two features of thermit welding allow the researcher great flexibility when constructing a model of heat transfer: a coordinate system can be chosen which facilitates description of the heat source, and coordinate movement need not be provided for.

A need to weld bars on thick plates (greater than 1/8 inch) is expected. Therefore, plate thickness must be included if any accuracy in predicting temperature history is to be expected, implying the need for a three dimensional model if Cartesian coordinates were selected. However, since this thesis is concerned with welding a bar or stud to a plate, the symmetry of the problem permits the selection of a cylindrical coordinate system. Only the dimensions "r" (radius) and "z" (thickness) can be used and still provide a complete description of heat flow.

Temperatures are expected to vary from approximately 40°F to 4000°F. For this reason, any model must consider material properties variable, specifically, thermal conductivity (k) and thermal diffusivity (α) in this case. Furthermore, in the model developed here, heat losses during

solidification are also taken into account. Since the welding is to be performed underwater, heat losses attributable to the environment must be considered. These include convection, boiling and radiation.

The following sections of this chapter present the governing differential equation, the finite difference reduction, the boundary conditions necessary for solution, and finally, the overall computer model.

B. HEAT FLOW EQUATION:

The general equation of heat flow without source terms and assuming conductivity to be independent of position is:[1]

$$\nabla^2 T = \frac{1}{\alpha}\cdot\frac{\partial T}{\partial t} \qquad \text{where } \alpha = \frac{k}{c\rho} \tag{2.1}$$

In cylindrical coordinates, if T is independent of θ, the equation appears as follows in partial differential notation:

$$\frac{\partial^2 T}{\partial r^2} + \frac{1}{r}\cdot\frac{\partial T}{\partial r} + \frac{\partial^2 T}{\partial z^2} = \frac{1}{\alpha}\cdot\frac{T}{t} \tag{2.2}$$

By separating the variables, the following solution can be obtained:[2]

$$T = [A\cdot e^{-\gamma^2\alpha t}]\cdot[B\cdot J_0(\zeta r) + C\cdot Y_0(\zeta r)] \cdot[D\cdot e^{-iz\sqrt{\gamma^2-\zeta^2}} + E\cdot e^{+iz\sqrt{\gamma^2-\zeta^2}}] \tag{2.3}$$

where A, B, C, D, E, γ and ζ are constants which must be evaluated by applying the appropriate boundary and initial conditions.

Unfortunately, the boundary conditions in this case are such that the constants cannot be evaluated. Therefore, the equation cannot be solved exactly, and a different approach must be used to predict temperature histories.

---

[1] See page 7 for definition of symbols.

[2] See Appendix A for detailed solution procedure.

C. FINITE DIFFERENCE SOLUTION:

Finite difference techniques can be applied to an unsteady-state conduction problem as long as the initial temperature distribution and boundary conditions are known.[3] This method is especially convenient when a digital computer is available.

First, a grid which describes the body in question is laid out as in Figure 7. A finite difference equation is then derived from the differential equation and is as follows:[4]

$$\frac{k\cdot(T_1 - T_0)\cdot 2\cdot\pi\cdot(r - r/2)\cdot\Delta z}{\Delta r} + \frac{k\cdot(T_2 - T_0)\cdot 2\cdot\pi\cdot r\cdot\Delta r}{\Delta z} +$$

$$\frac{k\cdot(T_3 - T_0)\cdot 2\cdot\pi\cdot(r + r/2)\cdot\Delta z}{\Delta r} + \frac{k\cdot(T_4 - T_0)\cdot 2\cdot\pi\cdot r\cdot\Delta r}{\Delta z}$$

$$= \frac{\rho\cdot c\cdot 2\cdot\pi\cdot r\cdot\Delta r\cdot\Delta z\cdot(T_0' - T_0)}{\Delta t} \qquad (2.4)$$

The above equation holds for any interior point in a two dimensional grid described by cylindrical coordinates (r and z). The equation is solved for the temperature (T_0') at one time interval (Δt) later and is as follows if $\Delta r = \Delta z = \delta$:

---

[3] See Kreith, Frank, Principles of Heat Transfer, International Textbook Co., Scranton, Pennsylvania, 1969; or Rohsenow, Warren M., and Choi, Harry, Heat, Mass, and Momentum Transfer, Prentice-Hall, Inc., Englewood Cliffs, New Jersey, 1965 for discussions of finite difference methods.

[4] For clarity, the equations in this section are written using numerical subscripts rather than alphabetic as in the computer program.

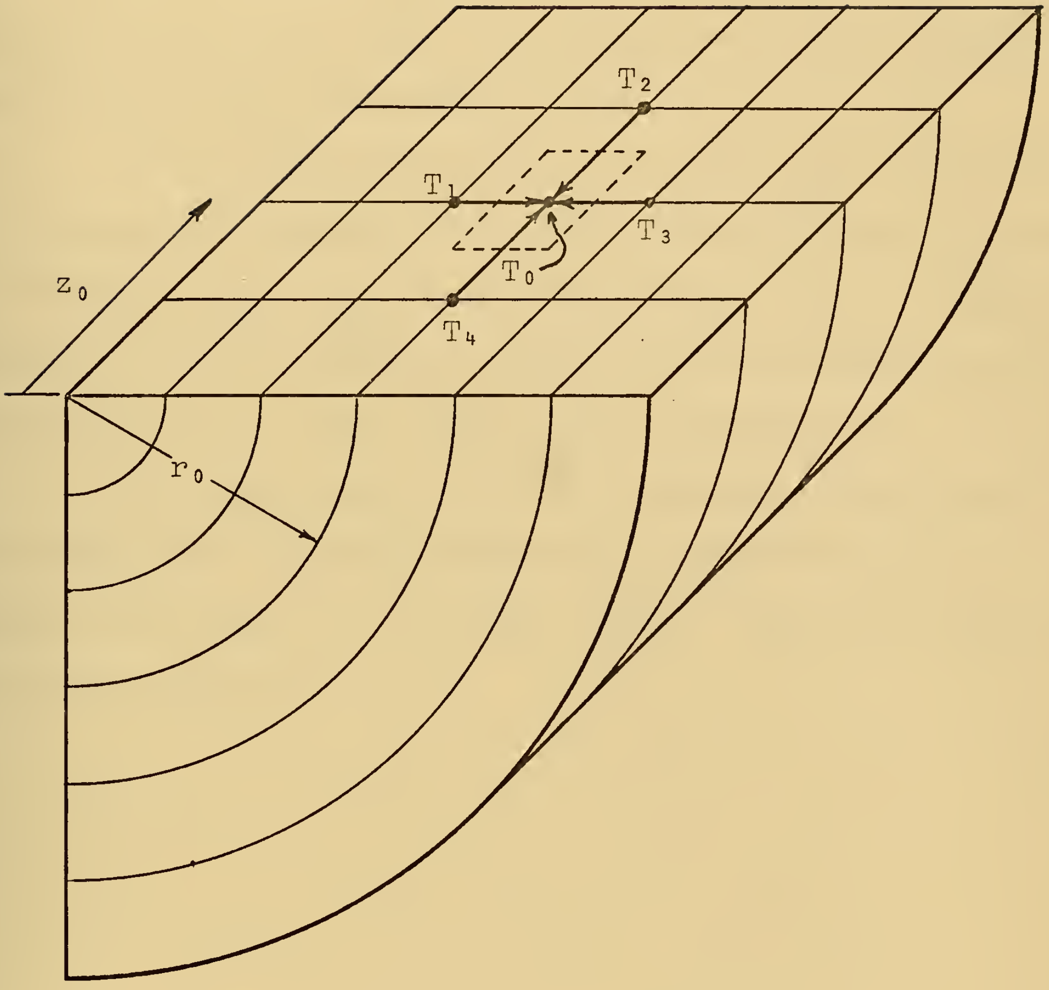

Figure 7: CYLINDRICAL GRID FOR FINITE DIFFERENCE COMPUTATION

$$T_0' = \frac{1}{M}\cdot[T_1\cdot(1 - s/(2\cdot r)) + T_2 + T_3\cdot(1 + s/(2\cdot r)) + T_4]+$$
$$(1 - 4/M)\cdot T_0$$

$$\text{where } M = \frac{s^2}{\alpha\cdot\Delta t}$$

In this case, M must be greater than 4 for the solution to converge. This infers that the selection of Δt is dependent upon grid size and the material used.

By applying the equation to every nodal point in the network, the temperature distribution at time $t + \Delta t$ can be determined from a given distribution at time t. Repeated application of the equation produces the temperature distribution at time $t + n\cdot\Delta t$, where n is an integer.

The equations for points located on the boundary of the body are somewhat different and depend upon the boundary conditions, i.e., heat losses. These are discussed in the next section.

D. HEAT LOSSES:

In this model, heat losses at the plate boundary are caused by convection, boiling, and radiation. However, unlike underwater arc and oxyacetylene welding, in this case, convection accounts for the majority of heat transfer to the environment. This is due to the thermit mold forming an effective insulation between areas of extremely high temperature and the environment.

When and if the surface temperature of portions of the plate in contact with water exceeds saturation temperature, nucleate boiling is also possible. This condition exists until the surface temperature of the plate reaches a point where an unstable vapor film covers the surface. At this point heat losses due to nucleate boiling reach a maximum; the point is sometimes referred to as that at which peak heat flux occurs. Subcooling of the environment tends to increase both the temperature of this point and the peak heat flux value, although literature search produced no studies which were directly applicable to this problem (pool boiling in subcooled water). However, the temperatures at the plate/water interface were not expected to reach peak heat flux level, and therefore, this point and further regimes of boiling (transition and film were not considered in this model.

When dealing with heat losses from a flat plate in the underwater environment, the orientation of the plate

is particularly important. As in most previous research on heat transfer in underwater welding, this study considers only horizontal plates.[5] But even in this restricted case; heat loss mechanisms on the bottom surface are different from those on the top. Differences in convection phenomena are clear. Heat fluxes attributable to convection are derived in Appendix B and summarized as follows:[6]

Top Plate Convection:

$$q_c/A = 32.2(T_{plate} - T_{water})^{4/3} \qquad [BTU/hr/ft^2] \qquad (2.6)$$

Bottom Plate Convection:

$$q_c/A = 12.2(T_{plate} - T_{water})^{5/4} \qquad [BTU/hr/ft^2] \qquad (2.7)$$

For nucleate boiling on the top surface, the correlation of experimental data presented by Rohsenow and Choi was considered to be valid within the accuracy required by this model.[7] Heat flux on the plate's top surface attributable to nucleate boiling is derived in Appendix B and is as follows:

Top Plate Nucleate Boiling:

$$q_b/A = 1.7494(T_{plate} - T_{sat})^3 \qquad [BTU/hr/ft^2] \qquad (2.8)$$

---

[5] For example, see Staub, James A., Fr., <u>Temperature Distribution in Thin Plates Welded Underwater</u>, Unpublished M.I.T. Engineers Thesis, June, 1971.

[6] See Kreith, op. cit., pp.

[7] See Rohsenow and Choi, op. cit., pp. 211 - 237.

However, this study hypothesizes that the above correlation does not hold for the bottom surface.[8] Since the plate is horizontal, bubble activity on the bottom surface is restricted, i.e., the normal boiling mechanism of bubble formation, collapse and ascent does not occur. What is hypothesized to occur is the formation of a semistable vapor film which effectively restricts heat transfer to a radiation mode. Since temperatures were not expected to be high enough for radiation to have any significant effect, the phenomenon is modeled as zero heat loss from areas on the bottom surface which are at a high enough temperature (T_{sat}) to produce the vapor film. In equation form:

Bottom Plate:

$$q_b/A = 0 \qquad (2.9)$$

$$q_r/A = 0 \qquad (2.10)$$

The total heat loss from either surface is simply the sum of the individual components as follows:

$$q/A)_{total} = q_c/A + q_b/A + q_r/A \qquad (2.11)$$

---

[8] Based in part on discussion with Warren M Rohsenow.

E. OVERALL MODEL AND COMPUTER SIMULATION:

As stated previously, since it is envisioned that a thermit welding device designed for underwater stud welding would be cylindrical in shape, at least in the area where it contacted the plate, cylindrical coordinates are used in the model. The thermit mixture is assumed to be reacted in a separate crucible and tapped into a space bounded by the plate, the stud, and the mold. Furthermore, no heat transfer is assumed to occur across the boundary between the plate surface and the mold. Figure 8 illustrates this model configuration.

The computerized model was developed to simulate temperature histories of points in the bar, plate, and weld metal as selected by a user. Since such information would be of long term use if underwater thermit welding were developed into an operational process, the computer program was written to be as general as possible. In this respect, a user is able to specify different materials (but limited to those where exothermic reactions are possible) and different geometries, e.g., plate thickness and stud radius, in addition to points for which temperature histories are desired.

As stated in a previous section of this chapter, the model is based on finite difference techniques. The model starts simulation at the time the crucible is tapped, permitting molten metal to enter the mold. The initial temperature of the molten metal is calculated based on the

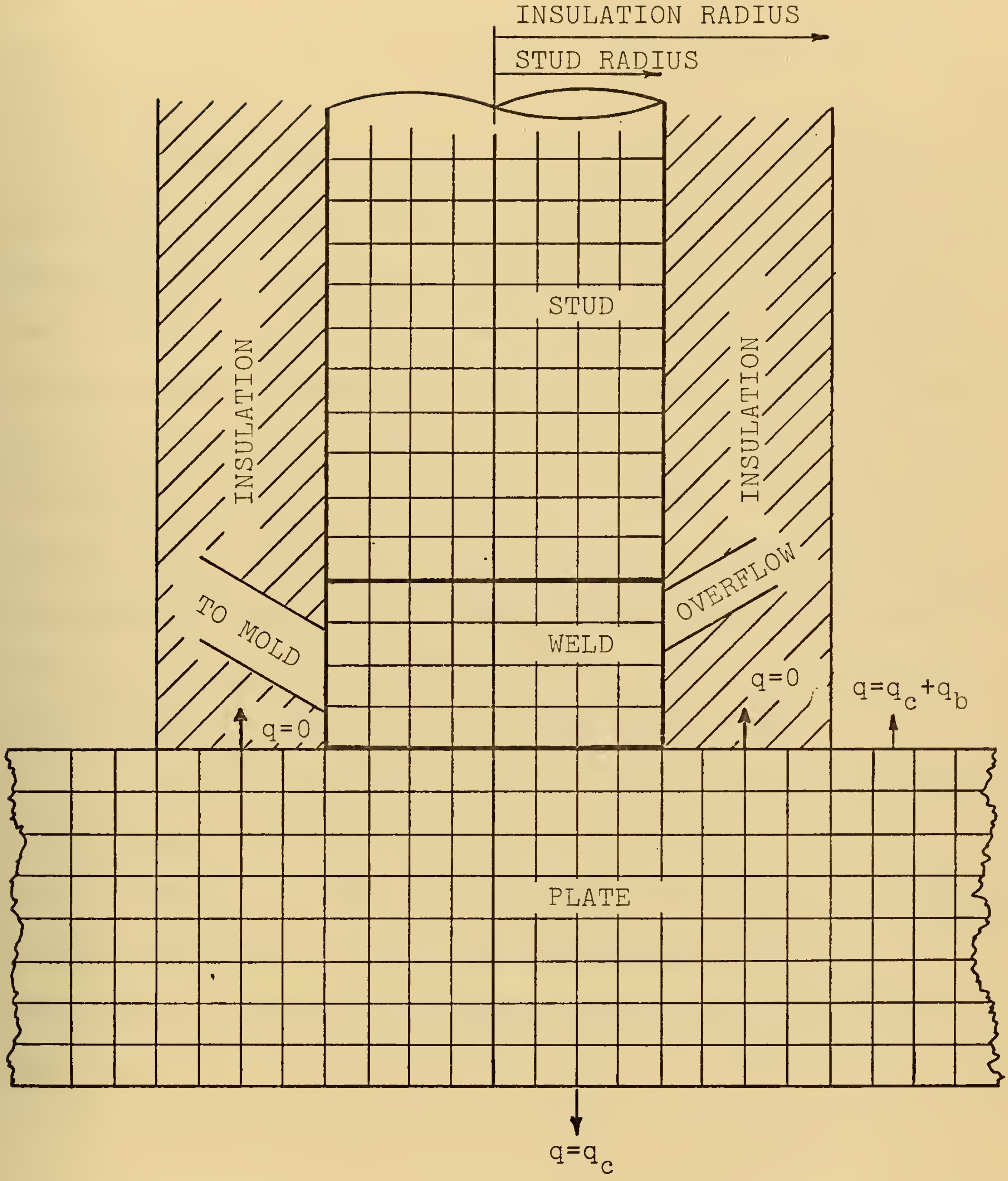

Figure 8: MODEL CONFIGURATION AND FINITE DIFFERENCE GRID

theoretical reaction temperature of the particular thermit mixture and the device efficiency. Flow through the mold is provided for.

Using these initial conditions and the environment temperature specified by the user, the model calculates temperatures at all nodal points one time increment later. Then the model uses these latest temperatures to calculate the next future temperature, and so forth until the desired simulation time (specified by the user) is completed. The variation of material properties (conductivity and diffusivity) with temperature and heat release during solidification are accounted for in the computations. Temperature histories for the ten selected points are printed showing temperatures for each second of simulation time.

Thus, the model steps its way through two indices: a space index and a time index. A simplified flow-chart is shown in Figure 9. The detailed-flow chart and the computer program, with sample input and output are included in Appendix D. Appendix C presents instructions for program use.

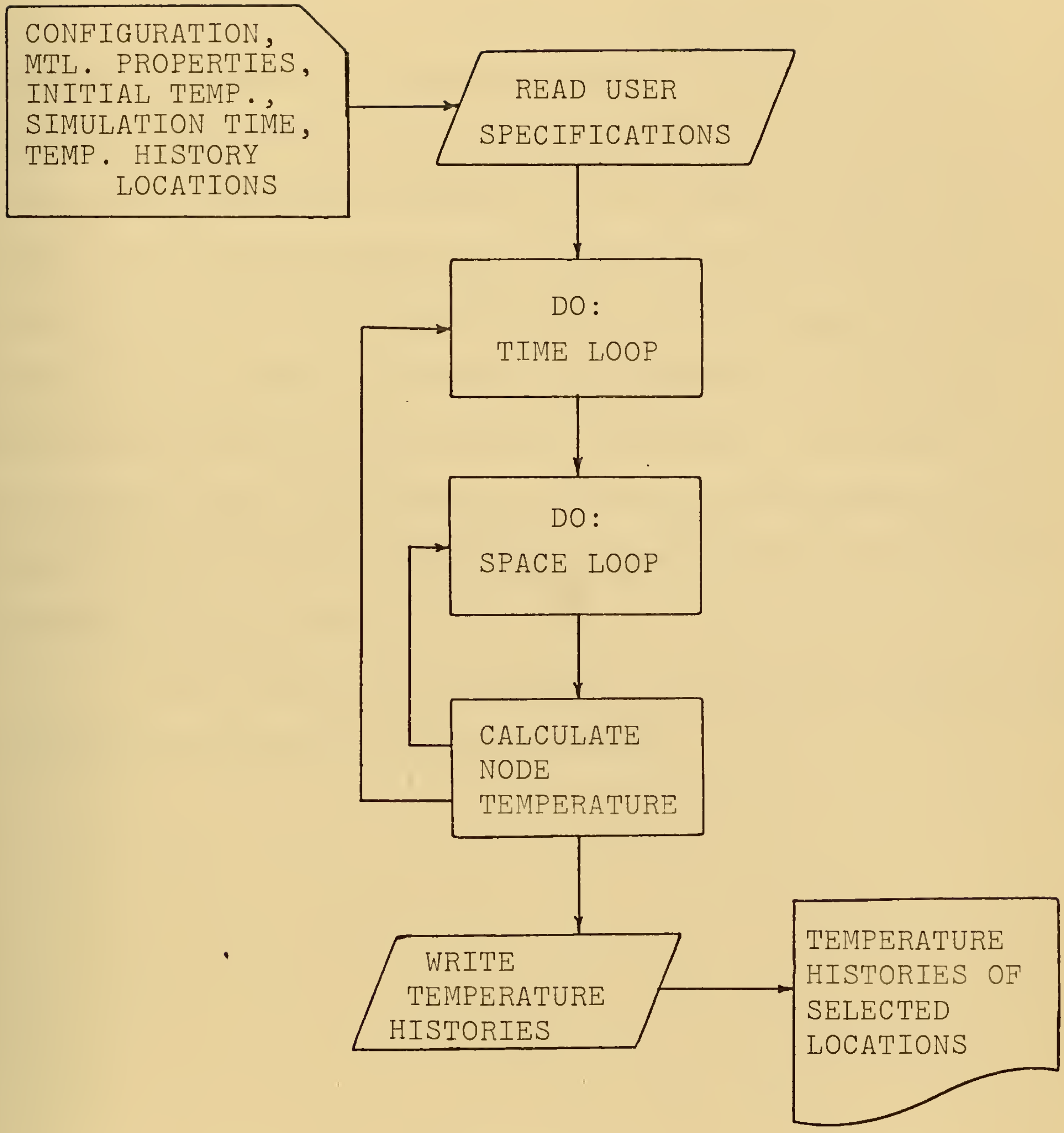

Figure 9: SIMPLIFIED FLOW-CHART OF HEAT FLOW SIMULATION

III. EXPERIMENTAL PROCEDURE

A. OVERVIEW:

As discussed in Chapter I, the experimental approach is related to three objectives of this thesis: first, determination of the moisture level which can be tolerated between the surfaces to be joined; second, the degree of surface contamination which can be effectively removed by flow of the molten metal itself between the surfaces to be joined; and third, verification of the model developed to predict temperature histories. In order to accomplish these objectives, a series of experiments was conducted utilizing a commercially available bar to plate thermit welding device.

The material and equipment used, and the procedures followed are discussed in this chapter.

B. EQUIPMENT AND MATERIAL:

The equipment and materials used are shown schematically in Figure 10 and are as follows:

1. Thermit welding device
2. Water tank
3. Temperature recorders
4. Thermocouples
5. Steel plate and bar
6. Support and hold down apparatus

A half-section of the thermit welding device used was shown in Figure 3 (Chapter I). The kit is designed for welding reinforcing bars to horizontal plates in air and is marketed by Thermex Metallurgical, Inc. of Lakehurst, New Jersey. This type of mold is fabricated using sand with a phenol-formaldehyde base resin as the bonding agent, and comes in two sections. The process is known as the "shell molding process." This type of mold is not reusable.

Other materials included in the kit include mild steel thermit welding compound (to match A.I.S.I. 1020 composition), tapping disks, starting thermit, sealing compound, molding sand, and bolts (for joining the two half-molds).

The thermit is reacted in a large chamber (on the left in Figure 3), and is tapped into the mold and between the surfaces to be joined. Flow of the molten metal continues up a riser and into an overflow chamber (on the right in Figure 3) until the equilibuium level is reached or

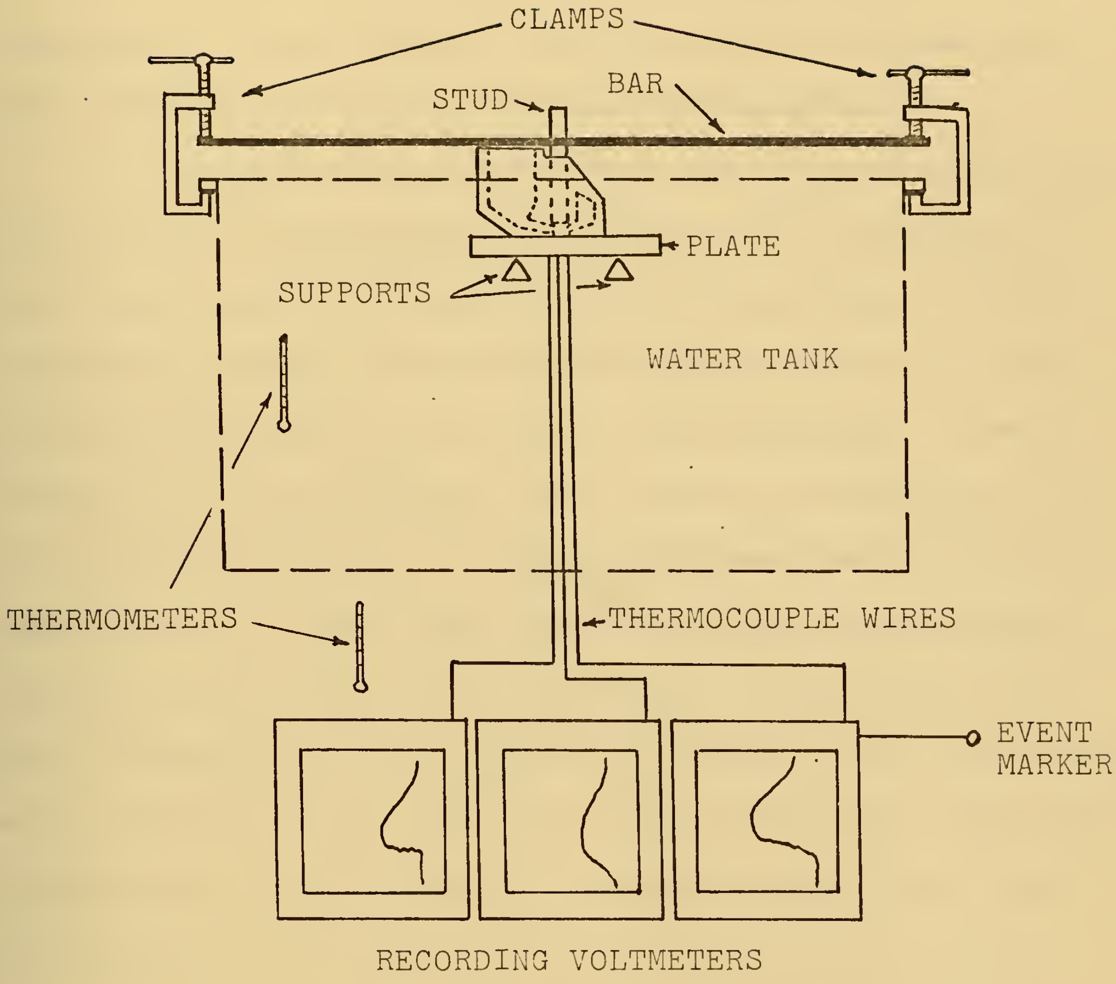

Figure 10: EQUIPMENT SCHEMATIC

solidification occurs.

A steel water tank measuring four feet in length, two feet in width, and three feet deep was used for the experiments. The tank was filled with ordinary tap water (Boston Ma.) and drained by gravity discharge.

Clevite Brush, Model 22, recording voltmeters were used to measure the output signal from the thermocouples. Three instruments were used for most experiments. Each instrument contained two channels so that a total of six thermocouples could be monitored simultaneously. Event markers on the instruments were connected electrically so that depressing a key on any one instrument would cause a simultaneous voltage signal to be recorded on all charts. Calibration was checked by inserting a thermocouple into known temperature baths (700°F and 1200°F). The instruments were adjusted so that chart velocity (horizontal scale) was 1 mm/sec, and one division on the chart paper's vertical scale equaled one milivolt (or, 50 mv for total scale).

Chromel-Alumel Type K, 0.020 inch diameter thermocouple wire was selected to measure temperature changes during welding. The size was considered more than adequate to withstand expected temperatures, and was governed primarily by the need for rapid response. In addition though, a small wire was considered desirable because thermocouples were to be installed by inserting and welding them into a hole drilled in the plate. Small holes were necessary to

limit inaccuracies introduced into the problem. Installation is covered in the next section of this chapter.

The plate and bar joined were mild steel (A.I.S.I. 1020 composition). The theoretical simulation model assumes a large plate. Therefore, the required length and width of the plate selected was based on the need to have little or no temperature change at the extremedies of the plate. A one foot square plate was expected to meet this requirement and was therefore selected. A thickness of one inch ($40^{\#}$ plate) was selected and considered satisfactory for verification of the model.

The plate was supported by a platform suspended from the sides of the tank. The mold was secured to the plate (held down) by a horizontal bar resting on top of the mold and clamped to the sides of the tank.

Ordinary mercury in glass thermometers were used to measure tank water temperature and the temperature of the thermocouple reference junction.

C. PROCEDURE:

1. Thermocouple Fabrication and Installation:

In order to avoid temperature gradients, the thermocouple's hot junction should be as small as possible. Ideally, it should be a point since we are,in effect, measuring a three dimensional distribution. Preparation of thermocouple hot junctions began with stripping two inches of insulation off the ends, and inserting them in 0.125 inch diameter, two hole ceramic insulators. The protruding ends were then twisted and fused together in an oxidizing oxyacetylene flame until only a small spherical shaped (0.030 to 0.040 inches in diameter) junction remained. Reference junctions were prepared in the same manner, only without the ceramic insulators.

Since it was necessary to obtain temperature histories of interior points in the plate, 0.128 inch diameter holes were drilled from the underside of the plate at desired radii to the desired depths. The temperature measurement locations are shown in Figure 11.

Intimate contact between the metal plate and the thermocouple was necessary in order to avoid unnecessary measurement inaccuracies. This was accomplished by welding the thermocouple junction to the base of the hole in the plate. The welding method employed utilized a capacitor discharge apparatus. Leads were connected to the thermocouple wires and the plate; the capacitor was charged; then

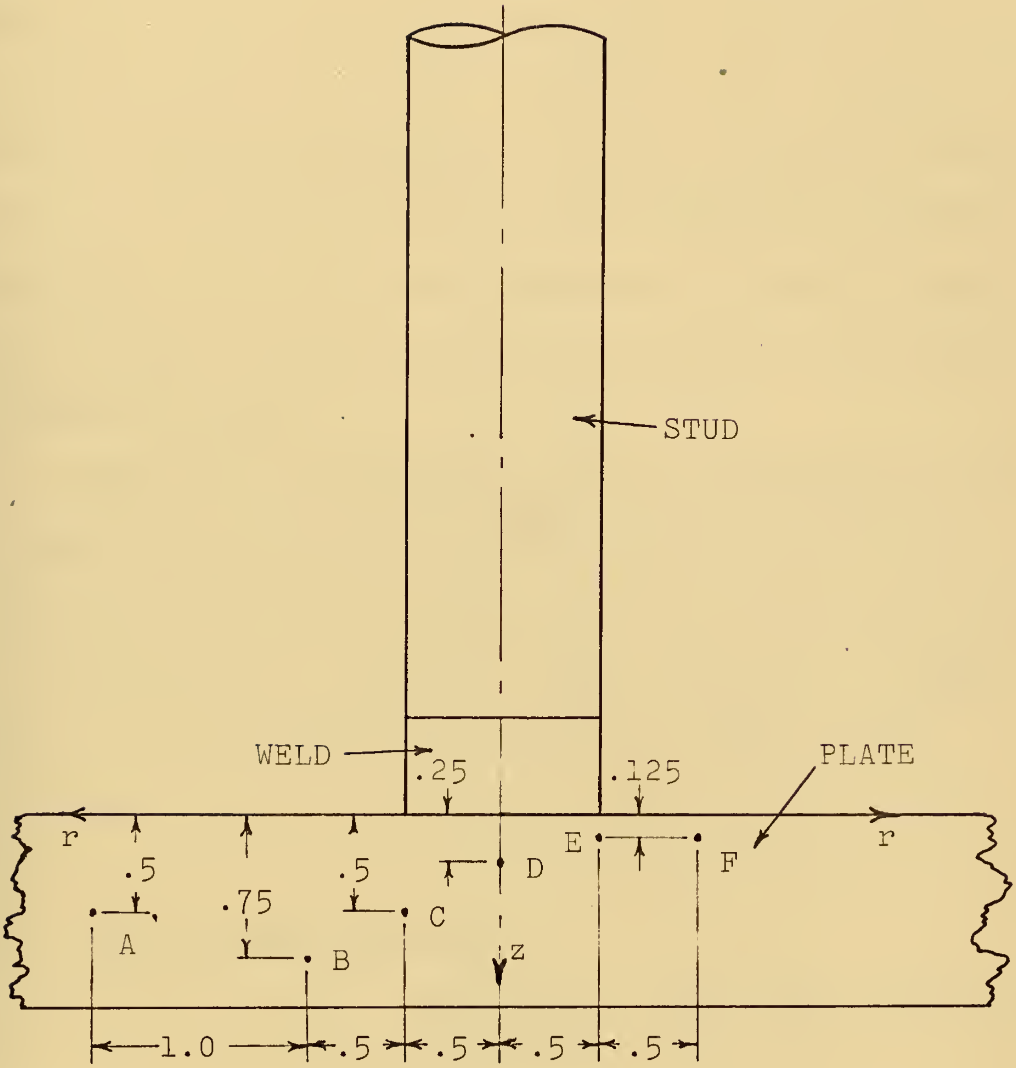

Scale: Full Size

Figure 11: THERMOCOUPLE LOCATIONS

the thermocouple was inserted into the plate to the base of the hole. The thermocouple was then withdrawn approximately 1/16 inch, and the capicitor dischared. An arc was struck between the plate and the thermocouple junction (detected audibly), and the thermocouple was again inserted all the way to the bottom of the hole. In each case, a weld of sufficient quality was achieved to obtain intimate contact between the thermocouple junction and the desired location in the plate. The joint was strengthened further by applying a ceramic cement (Sauereisen Sealing Cement) to the plate and ceramic insulator.

Since the entire plate would be underwater, the cement was waterproofed with a five percent acetic acid solution, and a four foot length of shrink tubing was shrunk onto the thermocouple wire and ceramic insulator. Figure 12 shows a section view of the completed thermocouple installation.

2. The Welding Operation:

A total of six experimental welds were performed. Of these, the first two were performed above water in a dry environment to ensure the equipment was functioning properly. The last four tests were performed underwater. It is the last four welds to which this section refers.

Prior to each actual welding operation, several preparatory steps were necessary. First, the mold was

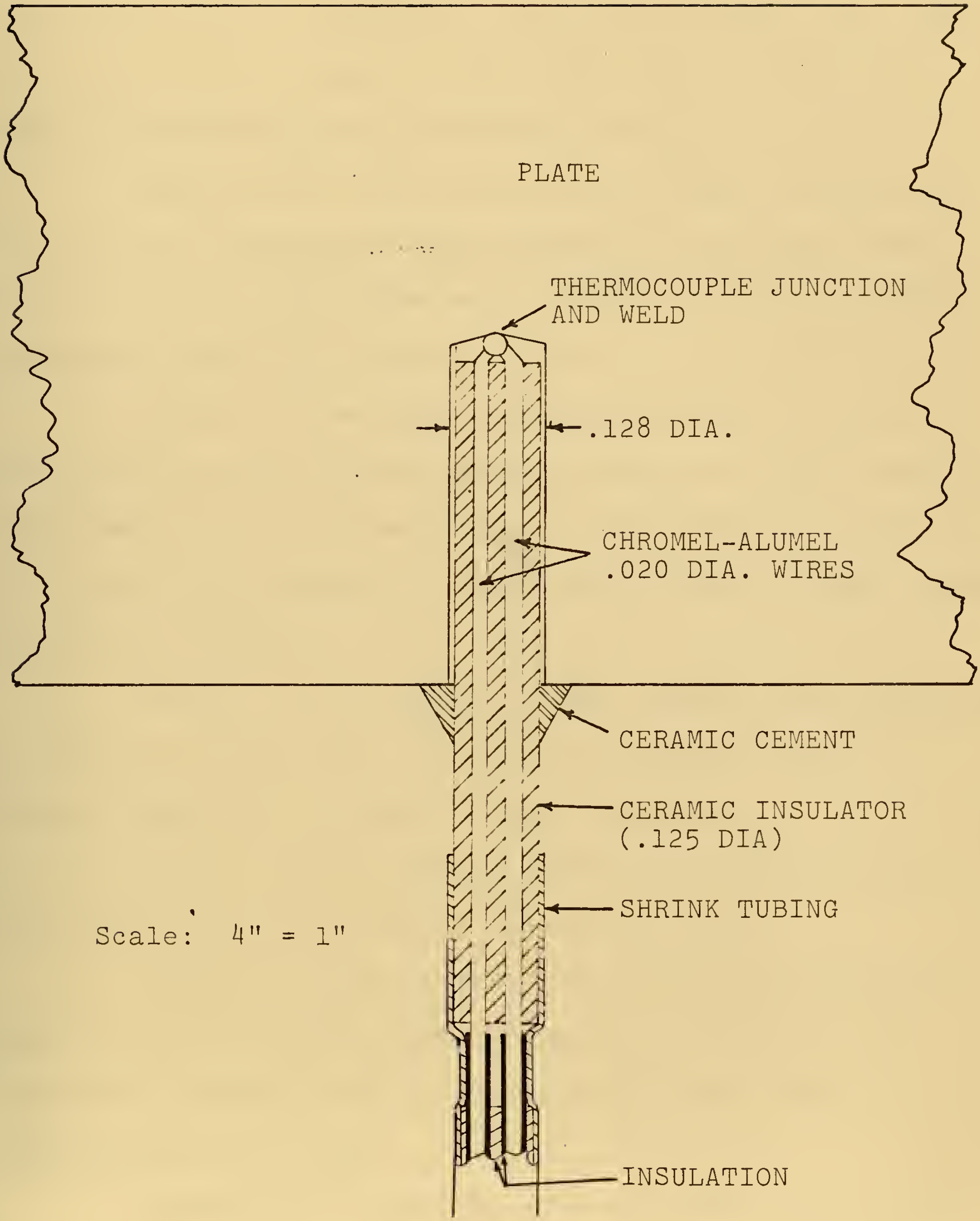

Figure 12: THERMOCOUPLE INSTALLATION

assembled, and the tapping disk inserted. Since one objective associated with the experiments was to determine allowable wetness level between the bar and the plate, each mold was sealed against leaks so that water level in the mold could be controlled, and therefore, known.

Second, the plate, with thermocouples installed, was placed on the supporting apparatus in the water tank. The thermocouple leads were then connected to the recording voltmeters (except in the last test).

Third, the welding device was positioned on the plate and vertical pressure applied via the bar and clamp arrangement. The reaction chamber of the mold was then filled with four pounds of thermit mixture and a small amount of starting thermit.

Fourth, the voltmeters were turned on and adjusted so that zero voltage was indicated while the plate was at ambient temperature (except in the last test).

Fifth, the tank was filled with water until the plate was four inches beneath the water surface.

Finally, after allowing sufficient time for the plate to attain thermal equilibrium with the water, the thermit was ignited with a oxyacetylene torch, and the welding operation begun.

Temperature histories were obtained in all underwater tests except the last. In each of the first three tests, a different wetness level between the bar and the

plate was created. The first underwater test was conducted with no water in the mold; the second was conducted with the mold 25% full of water; and the third was conducted with the mold 50% full of water. In each of the first three underwater tests, the surfaces to be joined were clean and free of oxidation.

The fourth and last underwater test, for reasons which will become apparent in the following chapter, was somewhat unique. The experiment was conducted with the mold 50% full of water, and on an oxidized plate surface. However, the major difference was the use of preheat. During device preparation, cavities were channeled in the device wall surrounding the mold. These cavities were filled with thermit which was ignited just before the thermit in the reaction chamber. The hypothesis was that by preheating the area to a high temperature, water within the mold would be vaporized and the actual welding would be performed in a nearly dry environment. No temperature measurements were conducted in this test.

In order to ascertain overall quality of welds, the last three specimens were subjected to tensile tests.

IV. RESULTS

A. HEAT FLOW:

In order to verify the computer simulation model, the points in the plate at which temperature histories were gathered matched those selected for simulation. Figures 13a through 13f are plots of experimental data vs. theoretical prediction curves. It is apparent from the figures that theoretical and experimental curves are quite close, thus validating the model as a prediction device.

The greatest variance exists between theory and experiment for points "C" and "E." Note from Figure 11 that these points lie directly beneath the weld/insulation boundary. The simulation models this boundary as a perfect insulator. However, the experimental device did not offer perfect insulation, and heat losses through it existed. For this reason, theoretical simulation predicted higher temperatures for points in close proximity to that boundary.

The model could have been changed to account for heat losses through the insulation boundary, but it is hypothesized that an actual device would offer better insulation than the one used for test purposes. Therefore, simulated temperatures would be in closer agreement with those achieved with an operational device, and the model was left unchanged.

Temperature history data tapes are included in Appendix E.

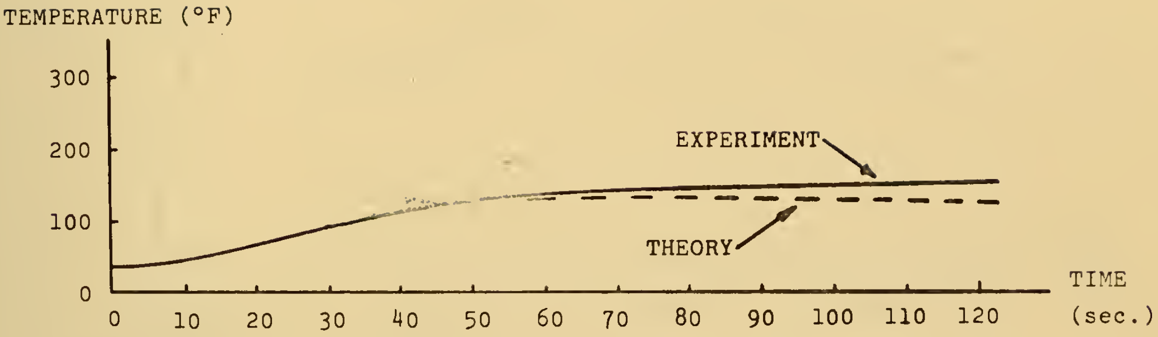

Figure 13a: TEMPERATURE HISTORY OF POINT "A"

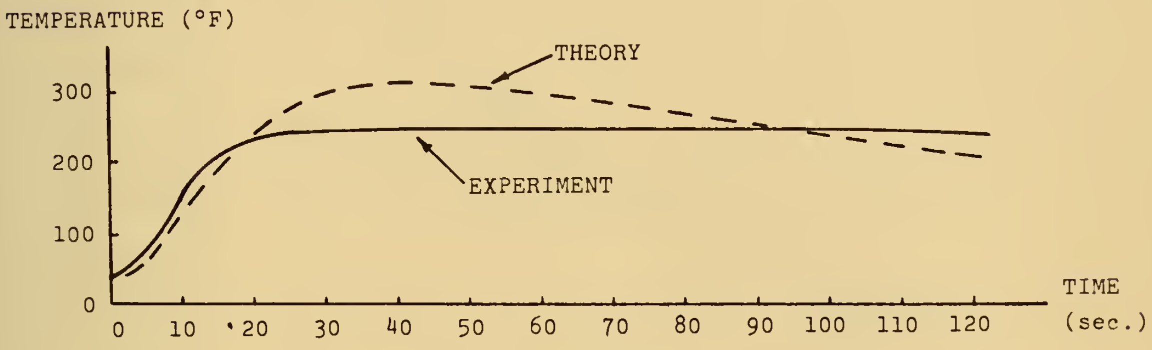

Figure 13b: TEMPERATURE HISTORY OF POINT "B"

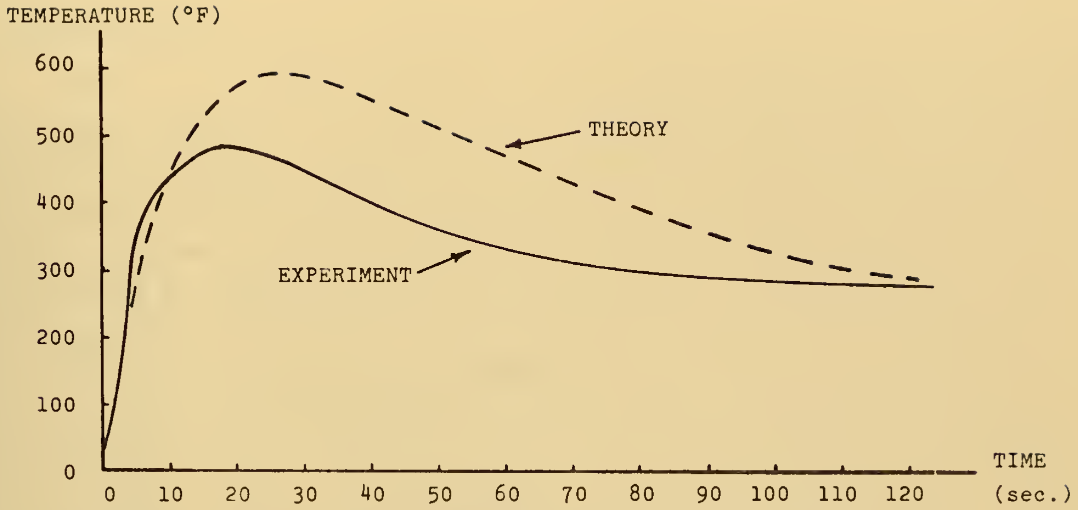

Figure 13c: TEMPERATURE HISTORY OF POINT "C"

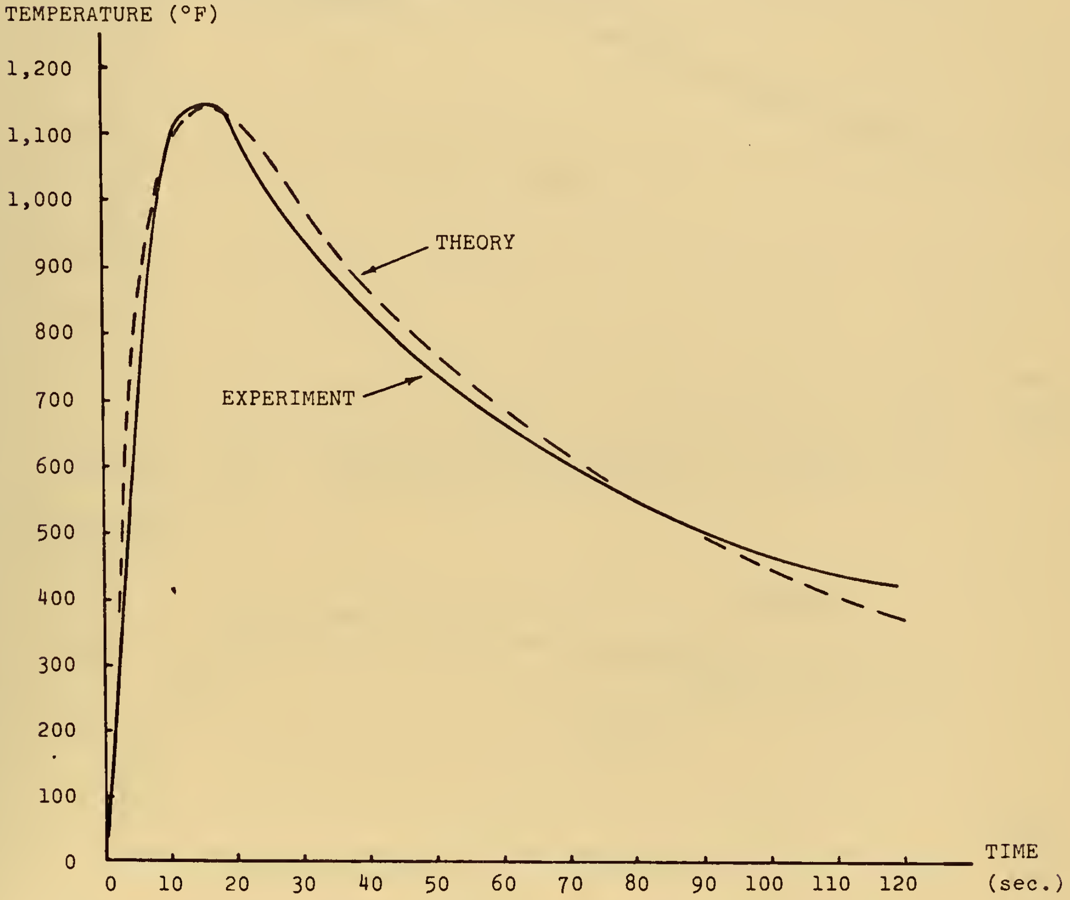

Figure 13d: TEMPERATURE HISTORY OF POINT "D"

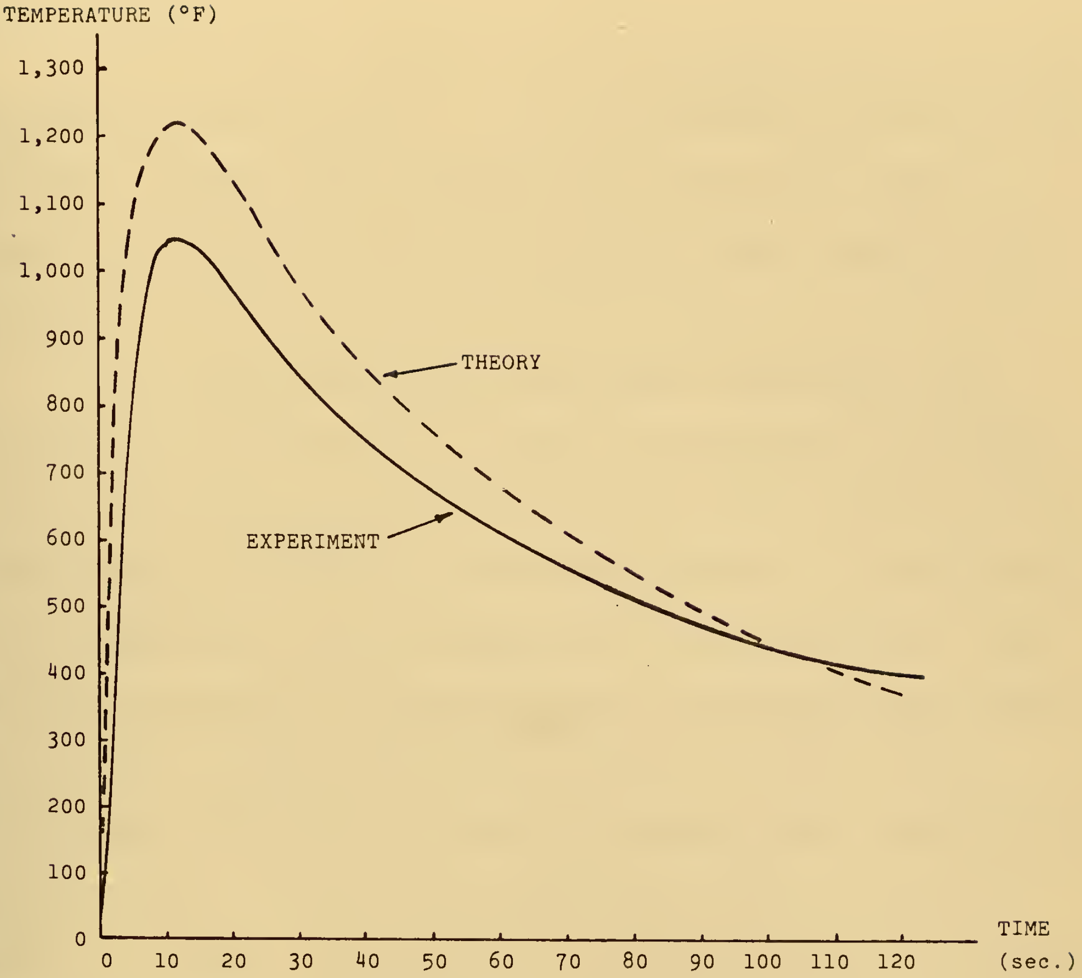

Figure 13e: TEMPERATURE HISTORY OF POINT "E"

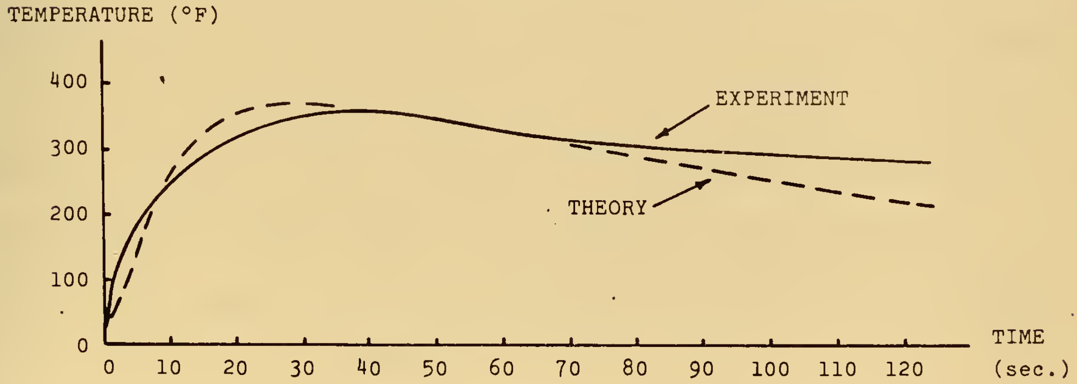

Figure 13f: TEMPERATURE HISTORY OF POINT "F"

B. WETNESS LEVEL:

Results with respect to an acceptable wetness level were somewhat disappointing. It was originally hypothesized that flow of molten metal through the mold would serve to evacuate any water present in the mold. This, however, did not occur.

In review, the first underwater experiment was conducted with no moisture or water in the mold; the second was conducted with the mold 25% full of water; and the third was conducted with the mold 50% full of water. In each case, a weld, externally sound in appearance, was achieved. However, when subjected to tensile tests, the second weld fractured at 25,000 pounds, and the third weld fractured at 12,000 pounds. Interiors of each of these latter two showed extreme porosity. The first underwater weld (dry mold) showed no porosity. Figure 14 illustrates predicted strength vs. wetness level for a one inch stud to plate weld (mild steel) based on this data, and in the absence of any preheat.

At this point I concluded that a sound underwater thermit bar to plate weld would not be possible unless a better method of evacuating any water in the mold were devised. The aspect of the experiment is discussed in the next section of this chapter.

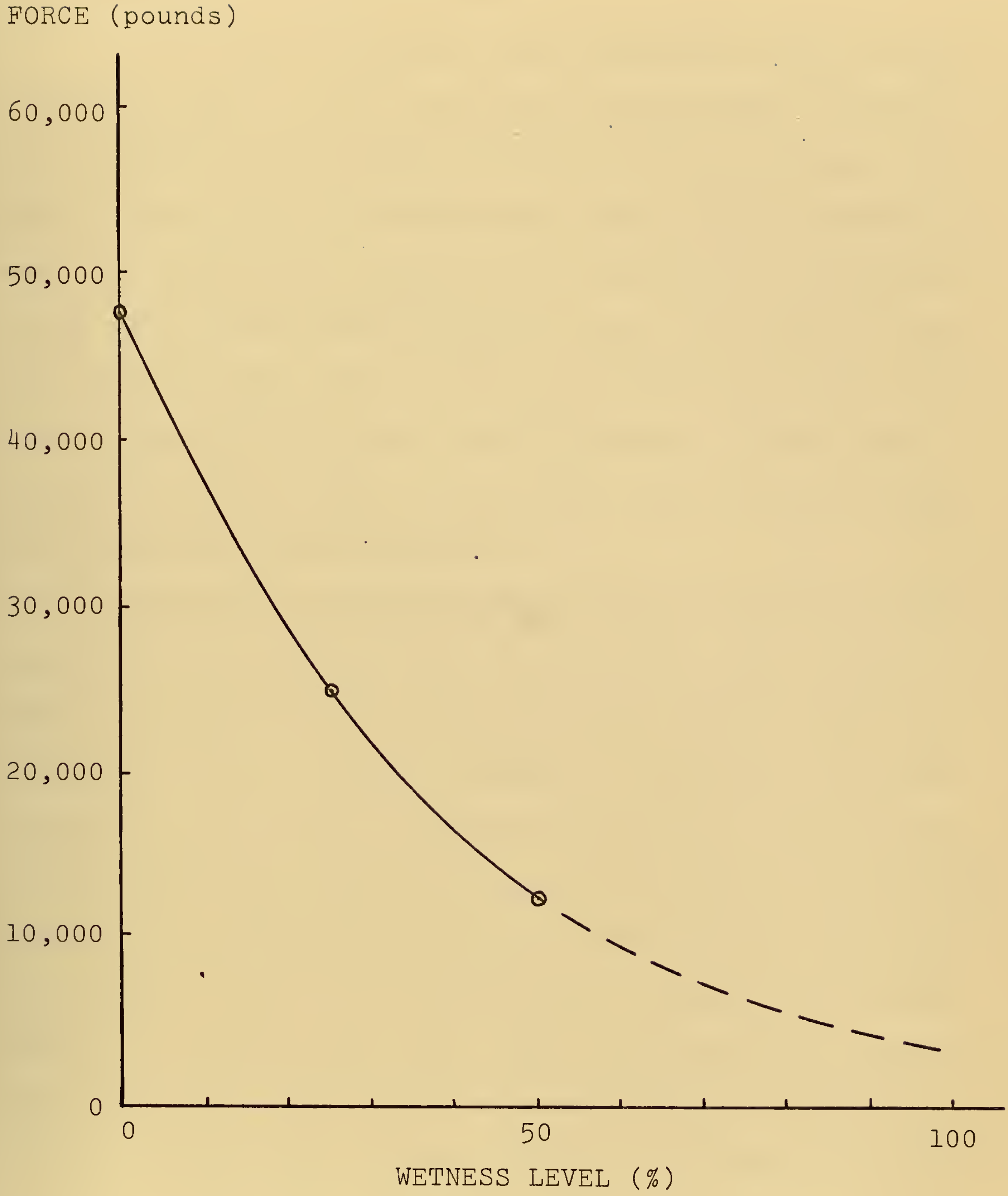

Figure 14: PREDICTED STRENGTH VS. WETNESS LEVEL

C. PREHEAT AND CLEANING ACTION:

The final experiment was conducted using the same procedures used in other underwater welds except for three differences: temperature measurements were not taken; the area of the plate to be welded was oxidized; and preheat was used. As explained in Chapter III, cavities were channeled in the device wall surrounding the mold, one cavity in each half of the device. Each cavity contained sufficient space for 0.25 cubic inch of the thermit mixture. Holes were drilled from above the intended water line to the cavities and filled with starting thermit.

After all other preparations had been made, including filling the mold half full of water, the thermit used for preheat was ignited immediately prior to igniting the thermit in the reaction chamber. Therefore, while the thermit in the reaction chamber was reacting, the water in the mold was being vaporized by the heat from the preheating thermit. Following the experiment, the weld was subjected to a tension test. At 44,400 pounds tension, the threaded portion of the bar fractured. This force was equivalent to subjecting the weld material to approximately 56,600 p.s.i.

Rather than subject the weld to further destructive mechanical tests, the bar and plate were split, and a specimen was polished and etched for visual examination. Figure 15 shows the entire weld area and portions of the plate and bar. The main features to note from the figure

are the lack of porosity in the weld and the excellent bonds achieved, even on the oxidized plate surface.

Figures 16a, b, c, and d provide closer looks at the specimen at low magnification (50X). Figure 16a shows the weld material itself; Figure 16b shows the fusion line; Figure 16c is a photograph of the heat affected zone; and Figure 16d shows the unaffected base metal in the plate.

Actually, there is evidence of a small porous area in the weld material. It is toward the upper right in Figure 15 and is shown under magnification (75X) in Figure 17. The small amount of porosity in this weld, however, is certainly encouraging at this stage of research.

Figure 15: CROSS SECTION OF THERMIT WELD MADE UNDERWATER USING PREHEAT (PLATE AT BOTTOM, 4X, 3% NITAL ETCH)

Figure 16a: MICROPHOTOGRAPH OF WELD MATERIAL (50X, 1% NITAL ETCH)

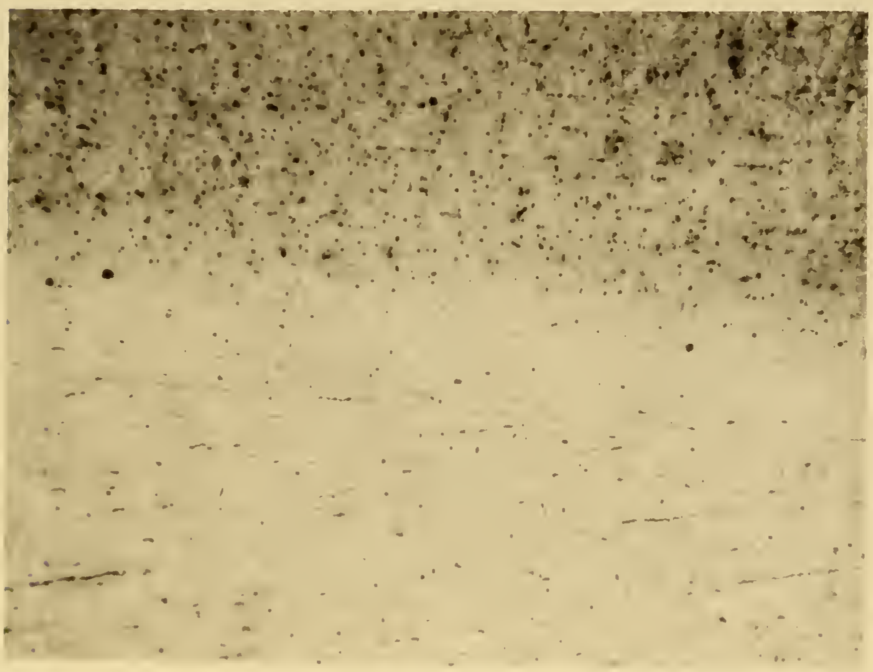

Figure 16b: MICROPHOTOGRAPH OF FUSION ZONE (50X, 1% NITAL ETCH)

Figure 16c: MICROPHOTOGRAPH OF HEAT AFFECTED ZONE (50X, 1% NITAL ETCH)

Figure 16d: MICROPHOTOGRAPH OF UNAFFECTED BASE METAL IN PLATE (50X, 1% NITAL ETCH)

Figure 17: MICROPHOTOGRAPH OF POROSITY IN WELD METAL (75X, 3% NITAL ETCH)

V. CONCEPTUAL DESIGN

A. GENERAL DISCUSSION:

As stated in Chapter I, the overall objective of this thesis is the conceptual design of a device which could be used to exothermicly weld a bar, stud, or padeye to underwater structures. The results presented in Chapter IV allow us to form important conclusions directly affecting device design. They are as follows:

1. Water must be removed from the weld area prior to tapping any molten metal into the area if a sound weld is to be achieved. It appears possible to accomplish this requirement through some means of preheating the area.

2. Flow of molten metal through the mold can effectively remove minor oxidation and dirt from the surfaces to be joined. Since no data was obtained on the removal of paint or more serious contamination, it is assumed for design purposes that flow of molten metal through the mold will not effectively remove anything more than minor oxidation and dirt.

3. Finally, and possibly most important, the success of the experiments demonstrates the feasibility of the process, thus implying that time spent on conceptual design and further development is not fruitless.

Device design is also guided by some basic

assumptions. The Navy's interest lies in salvaging or raising an object from the ocean floor. The device, therefore, should be operable at different (and deep) depths. Since the depths may exceed those reachable by a diver, the device should be remotely emplacable and operable through the use of a submersible. Furthermore, it is unrealistic to assume that the object has a horizontal surface on which to weld. For this reason, any device should be capable of operating at angles from zero to ninety degrees.

B. PRELIMINARY CALCULATIONS:

1. Size and Strength:

The original specifications of the Navy were that the padeye have a load carrying capability (L_y) of 50 tons or 112,000 pounds. Using a thermit mixture of mild steel composition assuming a yield strength (σ_y) of 60,000 p.s.i., the following calculations for the cross-sectional area (A) of the weld can be made.

$$L_y = A \cdot \sigma_y$$

$$A = L_y / \sigma_y = 112{,}000/60{,}000$$

$$A = 1.868 \text{ in.}$$

If the area is circular, this equates to a radius of 0.772 inches. Based on these figures, the load carrying portion of the total configuration was designed and is illustrated in Figure 18. The actual diameter of the area to be welded is 1.75 inches. Based on weld material strength of 60,000 p.s.i., this configuration would have a load carrying capability of 131,000 pounds or 58.6 tons.

2. Preheat:

A rather "make-shift" means of providing preheat was employed in the experimentation. Although special thermit mixtures exist specifically for providing preheat, previous research has indicated that another method may serve to not only accomplish this purpose but also remove

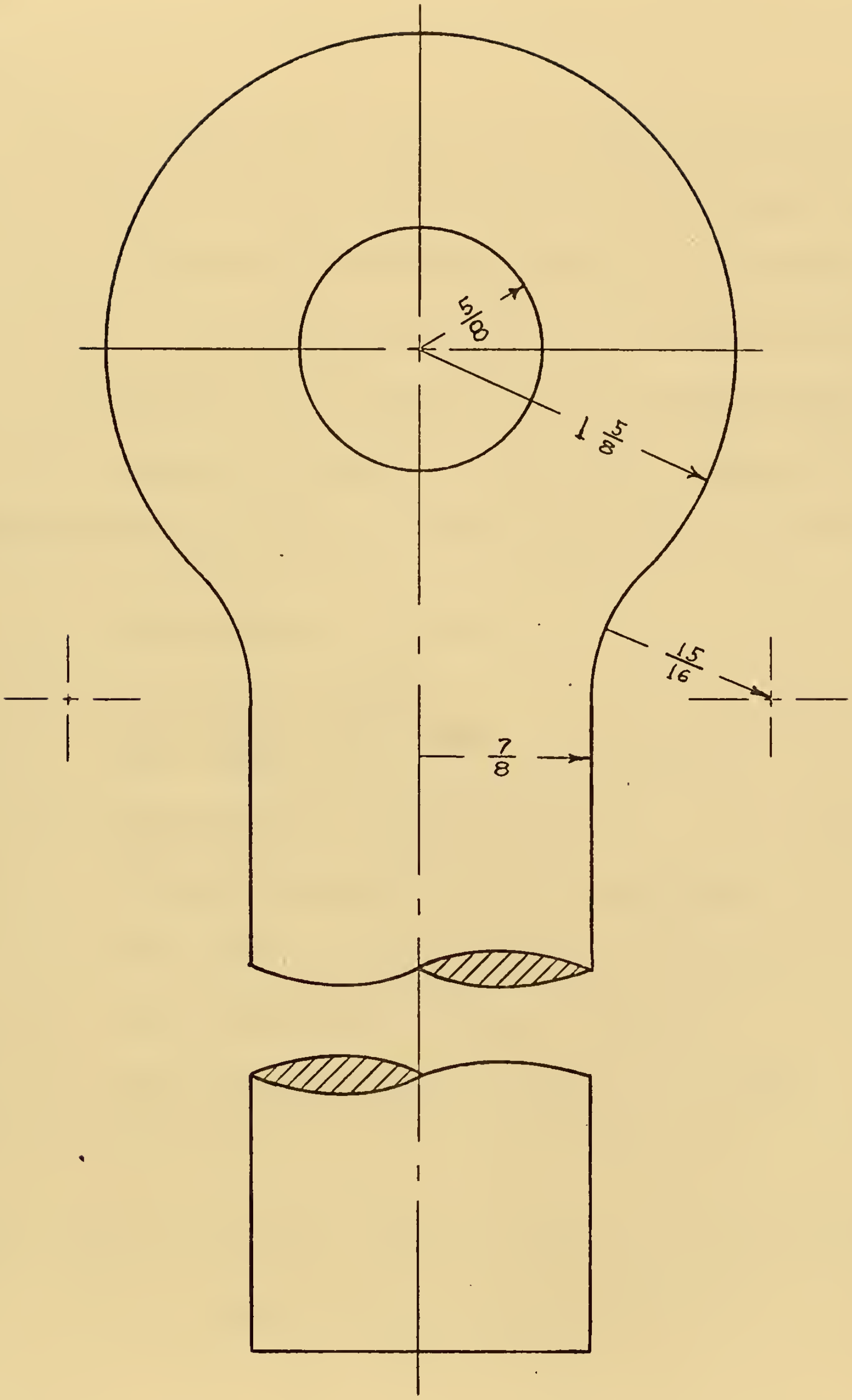

Figure 18: LOAD BEARING PORTION OF THERMIT WELDER

contaminants such as paint and minor marine growth from the plate surface.

This other method utilizes rocket technology.[9] The basic concept is that by exhausting high temperature gas into the weld area, both water removal and cleaning can be accomplished. An additional benefit is that some preheating of the parts to be joined is also accomplished.

The design is based on existing propellant composition, manufacturing methods, and assumptions as follows:

a. Propellant: Arcite 413A
b. Wired end burner
c. Mass flow rate $(\overset{\circ}{M}) = 1.7$ lb/sec
d. Density $(\rho) = 0.061$ lb/in^3
e. Chamber pressure $(P_c) = 2500$ psi
f. Burn rate (wired) $(r_b) = 1.8$ in/sec
g. Gas temperature $(T_{gas}) = 5000°F$
h. Ambient temperature $(T_{water}) = 40°F$
i. Desired burn time $(t_b) = 3.0$ sec

Given these specifications, grain diameter (D_g) and grain length (L_g) can be calculated as follows:[10]

---

[9] See Masubuchi, Koichi, Final Report on Underwater Thermit Welding of 50-Ton Padeye, Massachusetts Institute of Technology, October 29, 1971.

[10] Ibid., Appendix C, p. 4.

$$D_g = \sqrt{\frac{\overset{\circ}{M}}{(\pi/4)\cdot\rho\cdot r_b}} = \sqrt{\frac{4\cdot 1.7}{\pi\cdot 0.061\cdot 1.8}}$$

$$D_g = 4.42 \text{ in}$$

$$L_g = t_b\cdot r_b = 3.0\cdot 1.8$$

$$L_g = 5.4 \text{ in}$$

A grain of these dimensions weighs 5.05 pounds. According to Atlantic Research Corp., such a grain is easily manufactured within the present state-of-the-art.[11]

3. Pressure:

Present thermit welding devices used on the surface rely on gravity induced flow of the molten metal from the reaction chamber into the mold. Since in a device designed for underwater use the thermit reaction takes place in a chamber isolated from the environment, the molten metal must be forced into the mold area. None of the theoretical products of the thermit reaction are gaseous, and therefore, the pressure developed in the chamber upon reaction depends upon the temperature, pressure and volume of gas which was in the chamber prior to initiating the reaction. Although no specific calculations are presented here, the reaction chamber pressure requirements can be fulfilled prior to device emplacement based on temperature, volume and the specific gas used.

---

[11] Ibid., Appendix C, p. 4.

C. DESIGN:

A conceptual design was prepared based on results presented thus far in the thesis and is illustrated in Figure 19. The upper portion of the figure illustrates the device as it would be viewed from above while resting on a horizontal plate. Only the exterior outlines of the rocket propellant and thermit reaction chambers (right half of the view) are shown in this view. The lower portion of the figure shows a side section view.

The major portion of the device could be constructed from mild steel. The reaction chambers are of equal size and inclined at an angle of 45°. Each chamber is lined with a refractory such as magnesia. Ignition timing control and thermit chamber pressurizing apparatuses are located between the two chambers. Void volumes of the device are filled with insulating material and ballast to achieve the desired weight in water.

Perhaps the best way of explaining the device would be a discussion of its sequential operations. Before emplacing the device, and while still on the surface, the rocket propellant and thermit (6 pounds) are placed in the proper chambers, and the chambers sealed. The thermit chamber is then pressurized to a level dependent upon the depth of the intended weld, so that when the thermit reaction is complete, pressure equilibrium between the chamber and the environment will exist.

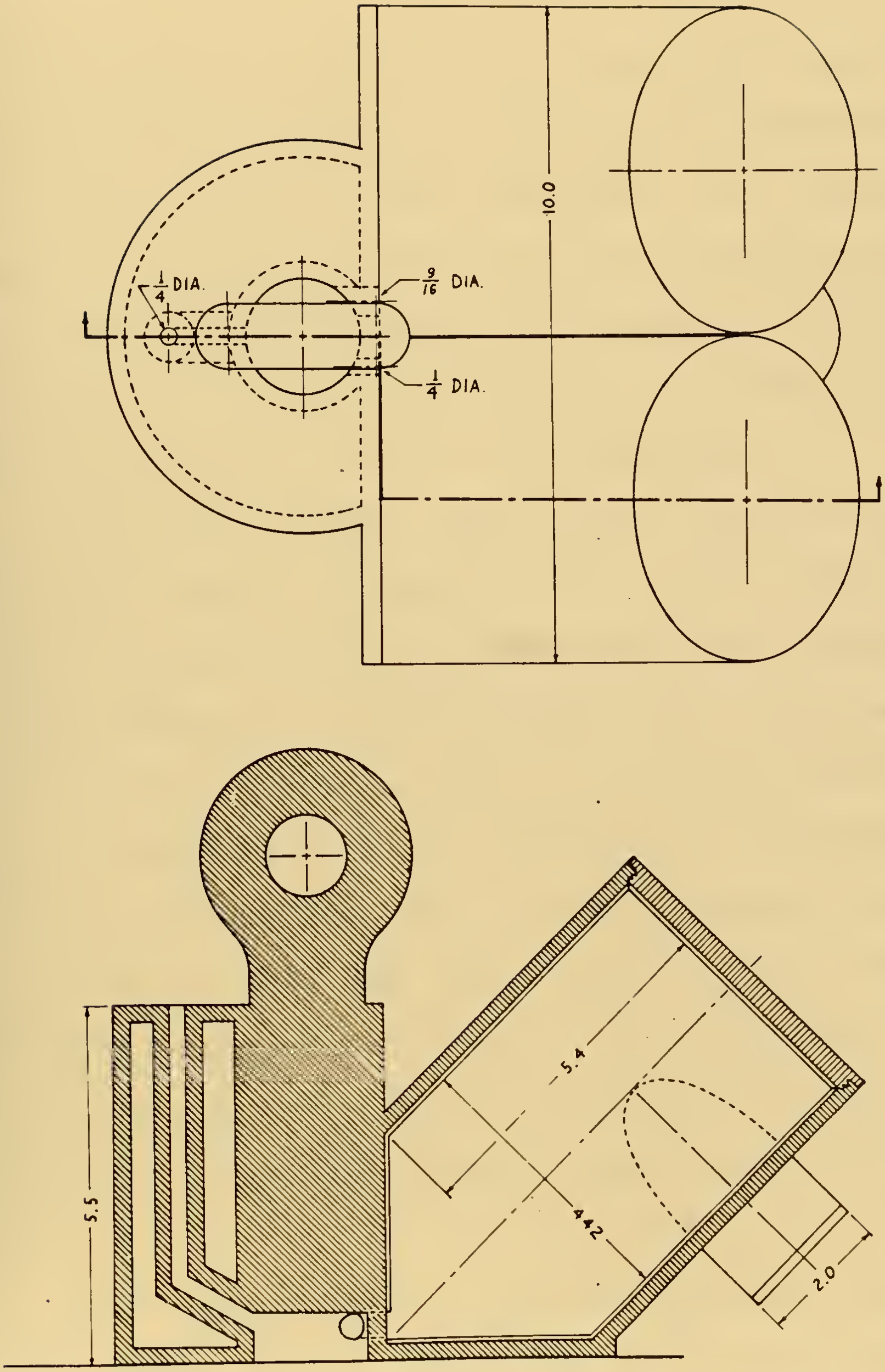

Figure 19: UNDERWATER THERMIT WELDER

The thermit reaction must be initiated first. Just prior to completion of the thermit reaction, the rocket propellant should be ignited. This timing and overall delay are controlled by the ignition timing control apparatus. However, at this writing, times reported in the literature to complete the thermit reaction are not accurate enough to state specific sequencing times. See Chapter VI for research recommendations. Suffice it to say at this point that the ignition timing control would be set and sealed.

The device is then emplaced by a diver or submersible with the reaction chambers on the "uphill" side if the object's surface is at an angle other than horizontal. Special appendages for handling purposes are not shown in Figure 19, but if attached, would not interfere with device operation. Temporary means of attaching an operational device until the weld is completed were not investigated and should be considered in any further study. The strength of any temporary bond need not be great, but only sufficient to hold the device in place until the reactions and the weld are completed. Adhesives or small thermit tack welds may suffice.

The timing mechanism first ignites the thermit. Fifteen to twenty seconds later, the rocket propellant is ignited, evacuating the water in the mold and vent riser, and preheating the area. When the propellant chamber pressure is in equilibrium with the environment pressure, the

molten metal is tapped into the mold. A portion of the metal continues up the vent riser and solidifies as it contacts the water, thus isolating the mold area from the water. The remaining metal seeks equilibuium between the propellant chamber and the thermit reaction chamber.

The gating is sized so that molten metal in the mold is always flowing under positive ferrostatic pressure. Since the chamber axes are at 45° to the object surface, this pressure will exist when welding at any angle from zero to ninety degrees.

Less than five minutes after the thermit reaction was initiated, the device should be capable of bearing the prescribed load. Due to time constraints, a test device could not be constructed, developed and tested as part of the thesis. Recommendations are contained in the following chapter.

VI. CONCLUSIONS AND RECOMMENDATIONS

A. CONCLUSIONS:

Perhaps the most signicicant conclusion arising out of this theses is that sound welds can be produced underwater by utilizing the thermit process. This was demonstrated by successfully welding a bar to a plate underwater.

However, several other important conclusions can be made. First, the accuracy of the temperature simulation model would seem to validate the hypothesis about heat losses underwater. More specifically, the boiling mechanisms on the bottom of a horizontal plate do not provide nearly as much heat transfer as boiling on top of the plate. Radiation through the vapor film would be the primary mechanism.

Second, a means of removing the water from between the surfaces to be joined must be incorporated in any thermit welding device destined for underwater use. Unless this is accomplished, porous welds can be expected.

Third, flow of molten metal through the mold can effectively remove minor oxidation and dirt from the surfaces to be joined.

B. RECOMMENDATIONS:

The first recommendation is related to underwater welding in general. If temperature simulation models are to become useful devices, more accurate definition of heat loss terms is essential. It is recommended that basic research be initiated on convection and pool boiling generated by a localized heat source on flat plates at all orientations.

The other recommendations contained herein are related specifically to underwater thermit welding. A requirement is envisioned for both academic and developmental work. Recommendations are as follows:

1. Construct and develop a device similar to that discussed in Chapter V. Several associated problem areas can be identified.

    a. Accurately define speeds of thermit reactions.
    b. Develop timing and ignition devices accordingly.
    c. Confirm sizing and arrangement of gating.
    d. Investigate methods of temporarily securing the device to a surface.
    e. Investigate dynamics of molten metal flow and pressure balances.

2. I believe the thermit process to be feasible for other underwater applications such as joining structures,

cables and pipe lines. Given this assumption, long term effort is implied. Development of other devices is essential. However, a most important research area lies in improving the properties of underwater thermit welds so that specifications of appropriate organizations and governing bodies can be met.

BIBLIOGRAPHY

1. AWS Welding Handbook, Sixth Edition, Chapter 57.

2. Kreith, Frank, Principles of Heat Transfer, International Textbook Co., Scranton, Pennsylvania, 1969.

3. Masubuchi, Koichi, Final Report on Underwater Thermit Welding of 50-Ton Padeye, Massuchusetts Institute of Technology, October, 1971.

4. Phillips, Arthur L., Ed., Modern Joining Processes, Chapter 10, AWS, New York, 1966.

5. Rohsenow, Warren M., and Choi, Harry, Heat, Mass, and Momentum Transfer, Prentice-Hall, Inc., Englewood Cliffs, New Jersey, 1965.

APPENDIX A

PARTICULAR SOLUTION TO HEAT FLOW EQUATION

The general equation is:

$$\nabla^2 T = \frac{1}{\alpha} \cdot \frac{\partial T}{\partial t}$$

Assuming temperature can be expressed as a product of time and space variables as follows:

$$T = U(r, z, \theta) \cdot \phi(t)$$

Then:

$$\nabla^2 T = \nabla^2 (U \cdot \phi) = \phi \cdot \nabla^2 U$$

and

$$\frac{\partial T}{\partial t} = U \cdot \frac{\partial \phi}{\partial t}$$

Therefore,

$$\phi \cdot \nabla^2 U = \frac{1}{\alpha} \cdot U \cdot \frac{\partial \phi}{\partial t}$$

and

$$\frac{\nabla^2 U}{U} = \frac{1}{\alpha \cdot \phi} \cdot \frac{\partial \phi}{\partial t} = -\gamma^2$$

where γ^2 is a constant.

Since ϕ is a function of t alone,

$$\frac{\partial \phi}{\partial t} = \frac{d\phi}{dt}$$

and

$$\frac{d\phi}{dt} + \gamma^2 \cdot \alpha \cdot \phi = 0$$

to which the solution is:

$$\underline{\underline{\phi = A\ e^{-\gamma^2 \alpha t}}}$$

where A is a constant.

Also,

$$\nabla^2 U + \gamma^2 U = 0$$

Assuming symmetry with respect to θ in cylindrical coordinates:

$$\nabla^2 U + \gamma^2 U = \frac{\partial^2 U}{\partial r^2} + \frac{1}{r}\cdot\frac{\partial U}{\partial r} + \frac{\partial^2 U}{\partial z^2} + \gamma^2 \cdot U = 0$$

Again assuming a product solution,

$$U = R(r)\cdot Z(z)$$

Since R is a function of r alone, and Z a function of z alone, it follows that:

$$Z\cdot\frac{\partial^2 R}{\partial r^2} + \frac{Z}{r}\cdot\frac{\partial R}{\partial r} + R\cdot\frac{\partial^2 Z}{\partial z^2} + \gamma^2\cdot R\cdot Z = 0$$

and

$$\frac{1}{R}\cdot\frac{d^2 R}{dr^2} + \frac{1}{R\cdot r}\cdot\frac{dR}{dr} = -\left(\frac{1}{Z}\cdot\frac{d^2 Z}{dz^2} + \gamma^2\right) = -\zeta^2$$

where ζ^2 is a constant.

Therefore:

$$r^2\cdot\frac{d^2 R}{dr^2} + r\cdot\frac{dR}{dr} + \zeta^2\cdot r^2\cdot R = 0$$

to which the solution is; (for $\zeta \neq 0$):

$$\underline{\underline{R = Z_0(\zeta r) = B\cdot J_0(\zeta r) + C\cdot Y_0(\zeta r)}}$$

where B and C are constants.

and,

$$\frac{d^2Z}{dz^2} + (\gamma^2 - \zeta^2)\cdot Z = 0$$

to which the solution is:

$$\underline{\underline{Z = D\cdot e^{-iz\sqrt{\gamma^2 - \zeta^2}} + E\cdot e^{iz\sqrt{\gamma^2 - \zeta^2}}}}$$

where D and E are constants.

Thus, the particular solution for temperature (T) is the product of the separated solutions:

$$T = \phi(t)\cdot R(r)\cdot Z(z)$$

or,

$$\underline{\underline{T = [A\cdot e^{-\gamma^2\alpha t}]\cdot[B\cdot J_0(\zeta r) + C\cdot Y_0(\zeta r)]}}$$
$$\underline{\underline{\cdot[D\cdot e^{-iz\sqrt{\gamma^2 - \zeta^2}} + E\cdot e^{iz\sqrt{\gamma^2 - \zeta^2}}]}}$$

where A, B, C, E, E, γ and ζ are constants which must be evaluated by applying the applicable boundary and initial conditions.

APPENDIX B

DERIVATION OF HEAT LOSS TERMS

1. Top of Plate Convection:

The following equation is recommended by McAdams for convection when the top surface of a horizontal plate is hot:[12]

$$\frac{h_c \cdot L}{k_\ell} = 0.14 \cdot (Gr_\ell \cdot Pr_\ell)^{1/3}$$

All properties for convection purposes were taken at 75°F and are as follows:

$$k_\ell = 0.35 \quad [BTU/hr/ft/°F]$$

$$Pr_\ell = 6.4$$

$$\frac{Gr_\ell}{L^3 \cdot \Delta T} = \frac{g \cdot \beta \cdot \rho^2}{\mu^2} = 4.4 \cdot 10^7 \quad [1/°F/ft^3]$$

where: g = acc. of gravity

ρ = density

β = coef. of expansion

μ = viscosity

L = length

$\Delta T = T_{plate} - T_{water}$

---

[12] See Kreith, *op. cit.*, p 340.

Substitution of these values into the convection equation yields:

$$h_c = 32.2 \cdot (T_{plate} - T_{water})^{1/3}$$

or

$$\underline{\underline{q_c/A = 32.2 \cdot (T_{plate} - T_{water})^{4/3} \quad [BTU/hr/ft^2]}}$$

2. Bottom of Plate Convection:

The recommended equation in this case is:[13]

$$\frac{h_c \cdot L}{k_\ell} = 0.27 \cdot (Gr_\ell \cdot Pr_\ell)^{1/4}$$

All properties are again taken at 75°F yielding the following result:

$$h_c = 12.2 \cdot (T_{plate} - T_{water})^{1/4}$$

or

$$\underline{\underline{q_c/A = 12.2 \cdot (T_{plate} - T_{water})^{5/4} \quad [BTU/hr/ft^2]}}$$

3. Top of Plate Nucleate Boiling:

The correlation presented by Rohsenow and Choi is as follows:

$$\frac{C_\ell \cdot \Delta T}{h_{fg} \cdot Pr_\ell^{1.7}} = C_{sf} \cdot \left(\frac{q_b/A}{\mu_\ell \cdot h_{fg}} \cdot \sqrt{\frac{g_0 \cdot \sigma}{g \cdot (\rho_\ell - \rho_v)}}\right)$$

---

[13] See Kreith, op. cit., p. 340.

Solving for q_b/A:[14]

$$q_b/A = \left(\frac{C_\ell \cdot \Delta T}{C_{sf} \cdot h_{fg} \cdot Pr_\ell^{1.7}}\right)^3 \cdot \frac{\mu_\ell \cdot h_{fg}}{\sqrt{\frac{g_0 \cdot \sigma}{g \cdot (\rho_\ell - \rho_v)}}}$$

Properties for nucleate boiling are taken at the saturation point (14.7 psia, 212°F) and are as follows:

C_ℓ = 1.021 BTU/lbm-°F

C_{sf} = 0.013

h_{fg} = 970.3 BTU/lbm

Pr_ℓ = 1.9

$g_0 = 4.17 \cdot 10^8$ lbm-ft/lbf-hr^2

$g = 4.17 \cdot 10^8$ ft/hr^2

ρ_ℓ = 59.8 lb/ft^3

ρ_v = 0.0372 lbm/ft^3

σ = 0.00404 lbf/ft

μ_ℓ = 0.74 lbm/hr-ft

Substitution of these values yields the following result:

$$\underline{\underline{q_b/A = 1.7494 \cdot (T_{plate} - T_{sat})^3 \quad [\text{BTU/hr/ft}^2]}}$$

---

[14] See Rohsenow and Choi, op. cit., p. 225.

APPENDIX C

INSTRUCTIONS FOR PROGRAM USE

The temperature simulation program has been written in FORTRAN language and can be executed without difficulty on any computer having a FORTRAN Compiler and 153,600 bytes of primary storage for use by the program. The user is required to furnish the following information describing the material, the environment, the device configuration, and the points for which temperature histories are desired:

1. First data card (FORMAT(4F10.4)):

   TENV: temperature of the water where the weld is to be made. [°F]

   TSAT: water saturation temperature at the depth the weld is to be made. [°F]

   TSOL: solidification temperature of the metal. [°F]

   THERM: theoretical reaction temperature. [°F]

2. Second data card (FORMAT (5F10.4))

   GAP: distance between the bar and the plate. [in]

   RBAR: radius of the bar. [in]

   RINS: radius of the insulation. [in]

   THICK: plate thickness. [in]

   EFF: theoretical or experimental device efficiency.

3. Third data card (FORMAT (2F10.4))

   RHO: density of metal at fusion temperature. [lbm/in^3]

   QFUS: latent heat of fusion of metal. [Btu/lbm]

4. Fourth data card (FORMAT (I3))

   IVAL: the number of data cards immediately following which describe thermal properties of the plate and bar. (maximum of 100)

5. Fifth group of data cards (FORMAT (3F10.5))

   TPROP: temperature at which particular property holds. [°R]

   CON: thermal concuctivity at temperature. [Btu/ft-hr-°R]

   DIF: thermal diffusivity at temperature. [ft/hr]

6. Next data card (actual number depends upon the number of cards describing properties) (FORMAT (2F10.4))

   TSIM: desired simulation time.[sec]

   FLOW: time of flow through the mold.[sec]

7. Next to last data card (FORMAT (12I5))

   Cylindrical coordinates of six points in the plate for which temperature histories are desired in the number of eighths of an inch a point is away from the center of the weld and plate top.

8. <u>Last data card</u> (FORMAT (4I5))

Coordinates of four points in the bar or weld material for which temperature histories are desired in the number of eighths of an inch a point is away fron the top of the plate.

APPENDIX D

PROGRAM FLOWCHART

PROGRAM LISTING

SAMPLE INPUT AND OUTPUT

```
04/27/72                                    AUTOFLOW CHART SET -      TEMPERATURE SIMULATION PROGR   PAGE  01

 CHART TITLE - INTRODUCTORY COMMENTS



                                  PROGRAM FOR PREDICTING TEMPERATURE DISTRIBUTIONS OF BAR T

                                  PLATE THERMIT WELD UNDERWATER
```

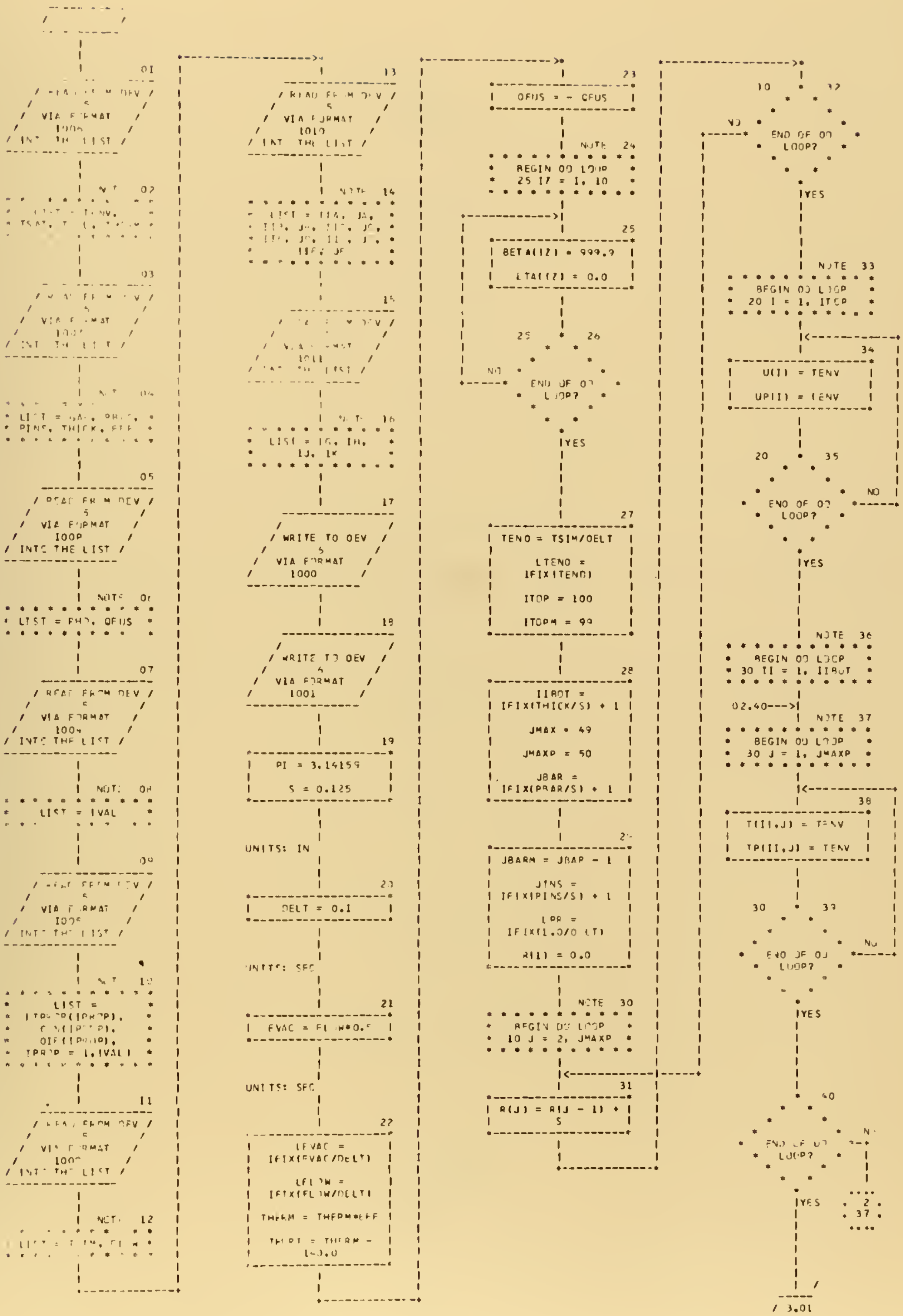
01
READ FROM DEV 5 VIA FORMAT 1006 INTO THE LIST
NOTE 02
LIST = TENV, TSAT, [illegible]
03
READ FROM DEV 5 VIA FORMAT [illegible] INTO THE LIST
NOTE 04
LIST = GAP, PRBAR, PINS, THICK, EFF
05
READ FROM DEV 5 VIA FORMAT 1008 INTO THE LIST
NOTE 06
LIST = PHO, OFUS
07
READ FROM DEV 5 VIA FORMAT 1004 INTO THE LIST
NOTE 08
LIST = IVAL
09
READ FROM DEV 5 VIA FORMAT 1005 INTO THE LIST
NOTE 10
LIST = (TPROP(IPROP), CON(IPROP), DIF(IPROP), IPROP = 1, IVAL)
11
READ FROM DEV 5 VIA FORMAT 1007 INTO THE LIST
NOTE 12
LIST = TIM, FLOW
13
READ FROM DEV 5 VIA FORMAT 1010 INTO THE LIST
NOTE 14
LIST = IIA, JA, IIB, JB, IIC, JC, IID, JD, II, J, IIE, JE
15
READ FROM DEV 5 VIA FORMAT 1011 INTO THE LIST
NOTE 16
LIST = IG, IH, IJ, IK
17
WRITE TO DEV 6 VIA FORMAT 1000
18
WRITE TO DEV 6 VIA FORMAT 1001
19
PI = 3.14159
S = 0.125
UNITS: IN
20
DELT = 0.1
UNITS: SEC
21
EVAC = FLOW*0.5
UNITS: SEC
22
LEVAC = IFIX(EVAC/DELT)
LFLOW = IFIX(FLOW/DELT)
THERM = THERM*EFF
THERT = THERM - 140.0
23
OFUS = - OFUS
NOTE 24
BEGIN DO LOOP 25 IZ = 1, 10
25
BETA(IZ) = 999.9
ETA(IZ) = 0.0
25 26
NO
END OF DO LOOP?
YES
27
TENO = TSIM/DELT
LTENO = IFIX(TENO)
ITOP = 100
ITOPM = 99
28
IIBOT = IFIX(THICK/S) + 1
JMAX = 49
JMAXP = 50
JBAR = IFIX(PRBAR/S) + 1
29
JBARM = JBAR - 1
JINS = IFIX(PINS/S) + 1
LPR = IFIX(1.0/DELT)
R(1) = 0.0
NOTE 30
BEGIN DO LOOP 10 J = 2, JMAXP
31
R(J) = R(J - 1) + S
10 32
NO
END OF DO LOOP?
YES
NOTE 33
BEGIN DO LOOP 20 I = 1, ITOP
34
U(I) = TENV
UP(I) = TENV
20 35
NO
END OF DO LOOP?
YES
NOTE 36
BEGIN DO LOOP 30 II = 1, IIBOT
02.40--->
NOTE 37
BEGIN DO LOOP 30 J = 1, JMAXP
38
T(II,J) = TENV
TP(II,J) = TENV
30 39
NO
END OF DO LOOP?
YES
40
NO
END OF DO LOOP?
YES
2
37
3.01

CHART TITLE - PROCEDURES

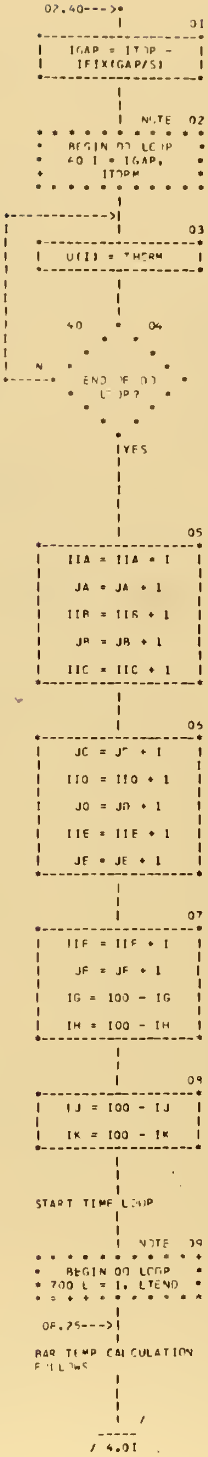

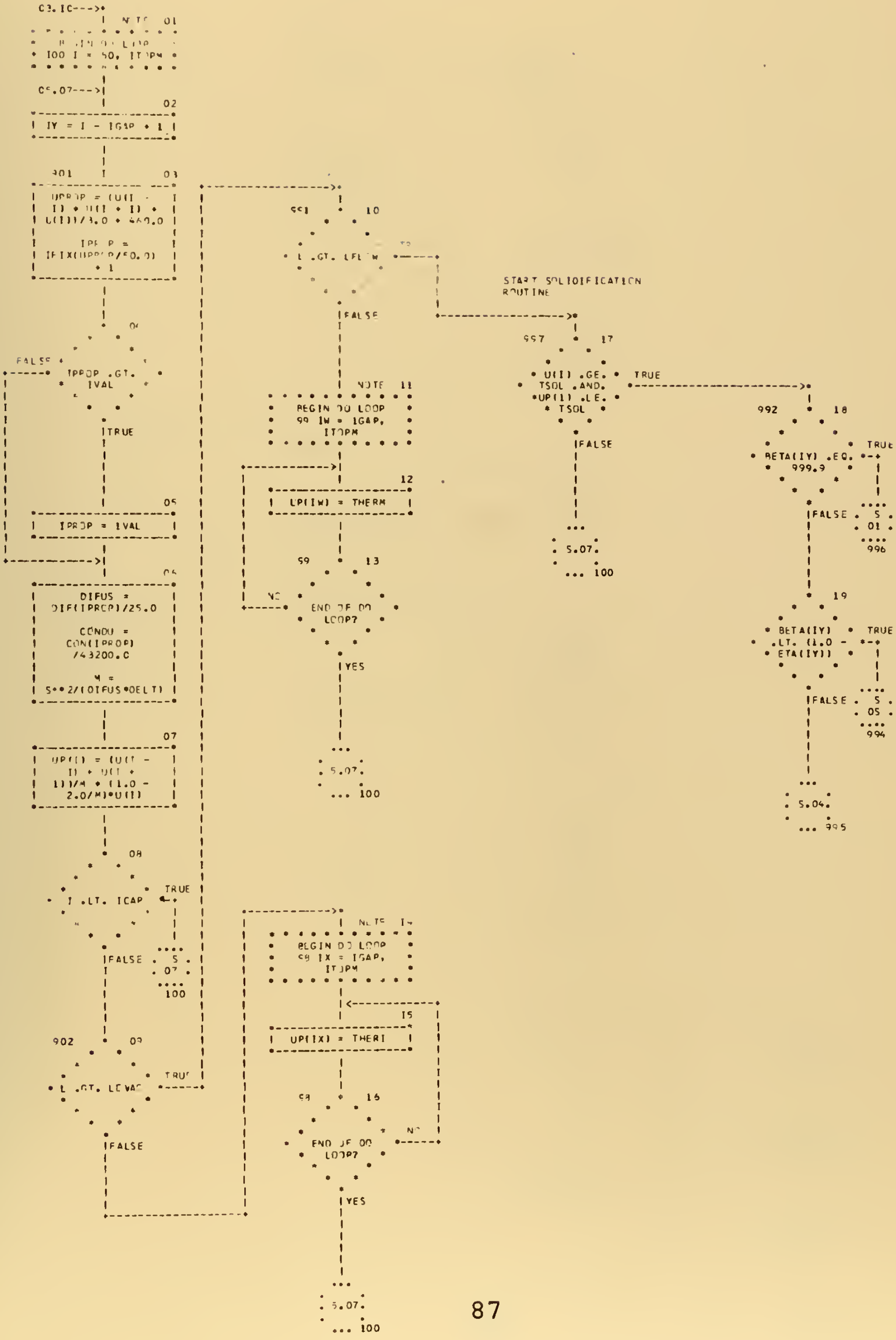
03.10--->
NOTE 01
BEGIN DO LOOP
100 I = 50, ITOPM
05.07--->
02
IY = I - IGAP + 1
901 03
UPROP = (U(I - 1) + U(I + 1) + U(I))/3.0 + 460.0
IPROP = IFIX(UPROP/50.0) + 1
04
FALSE
IPROP .GT. IVAL
TRUE
05
IPROP = IVAL
06
DIFUS = DIF(IPROP)/25.0
CONDU = CON(IPROP) /43200.0
M = S**2/(DIFUS*DELT)
07
UP(I) = (U(I - 1) + U(I + 1))/M + (1.0 - 2.0/M)*U(I)
08
I .LT. ICAP
TRUE
FALSE
S. 07.
100
902 09
L .GT. LEVAC
TRUE
FALSE
551 10
L .GT. LFLOW
TO
FALSE
NOTE 11
BEGIN DO LOOP
99 IW = IGAP, ITOPM
12
UP(IW) = THERM
99 13
NO
END OF DO LOOP?
YES
5.07.
100
NOTE 14
BEGIN DO LOOP
98 IX = IGAP, ITOPM
15
UP(IX) = THERI
98 16
NO
END OF DO LOOP?
YES
5.07.
100
START SOLIDIFICATION ROUTINE
997 17
U(I) .GE. TSOL .AND. UP(I) .LE. TSOL
TRUE
FALSE
5.07.
100
992 18
BETA(IY) .EQ. 999.9
TRUE
FALSE
S. 01.
996
19
BETA(IY) .LT. (1.0 - ETA(IY))
TRUE
FALSE
S. 05.
994
5.04.
995

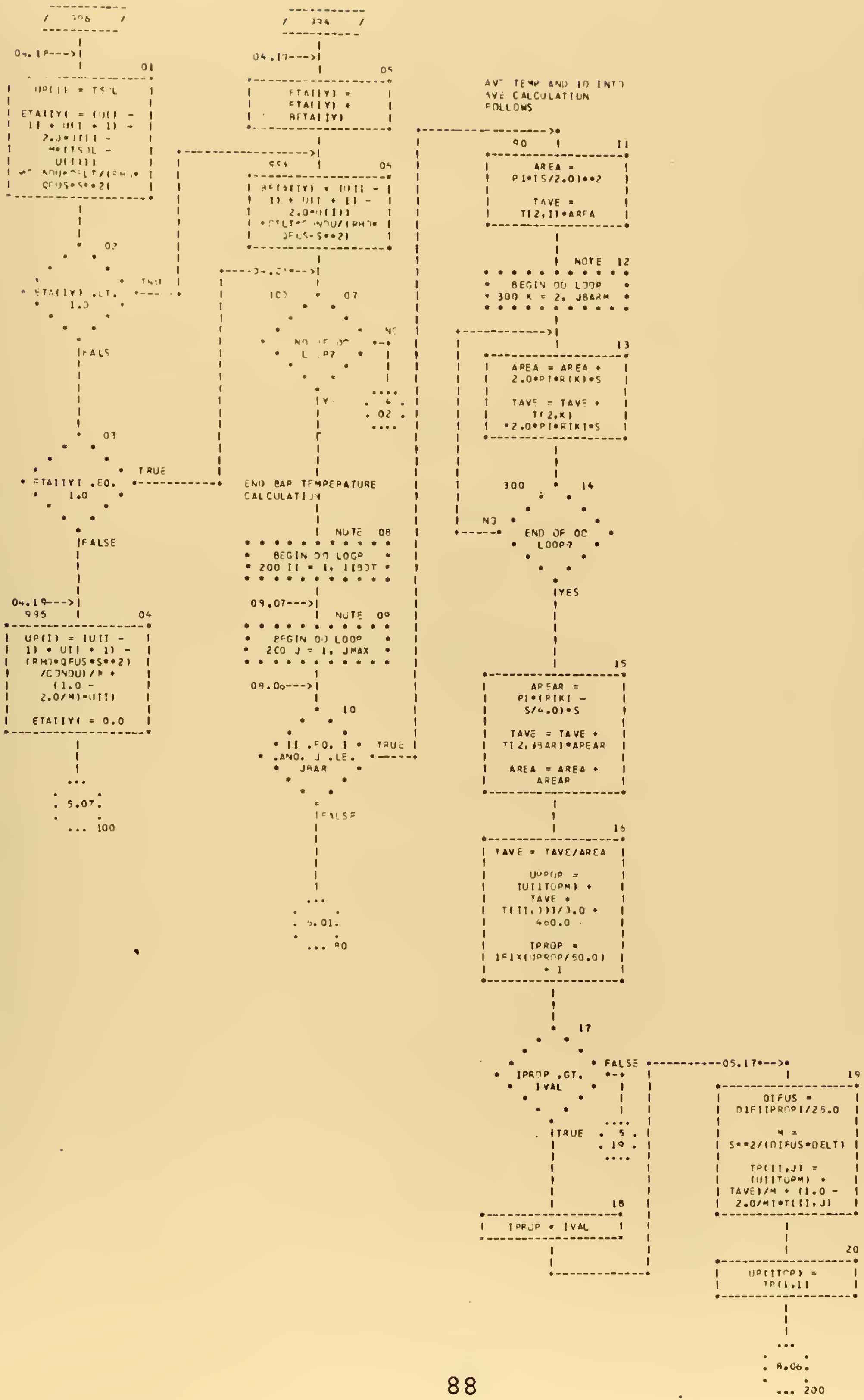

996
04.18--->
01
UP(1) = TSOL
ETA(IY) = (U(I - 1) + U(I + 1) - 2.0*U(I) - M*(TSOL - U(I)))*CONDU*DELT/(RHO*QFUS*S**2)
02
ETA(IY) .LT. 1.0
TRUE
FALSE
03
ETA(IY) .EQ. 1.0
TRUE
FALSE
04.19--->
995
04
UP(I) = (U(I - 1) + U(I + 1) - (RHO*QFUS*S**2)/CONDU)/M + (1.0 - 2.0/M)*U(I)
ETA(IY) = 0.0
5.07.
100
994
04.17--->
05
ETA(IY) = ETA(IY) + BETA(IY)
994
06
BETA(IY) = (U(I - 1) + U(I + 1) - 2.0*U(I)) *DELT*CONDU/(RHO*QFUS*S**2)
09.07--->
100
07
NO. OF DO LOOP?
NO
4.02
YES
END BAR TEMPERATURE CALCULATION
NOTE 08
BEGIN DO LOOP 200 II = 1, IBOT
09.07--->
NOTE 09
BEGIN DO LOOP 200 J = 1, JMAX
08.06--->
10
II .EQ. I .AND. J .LE. JBAR
TRUE
FALSE
5.01.
80
AVE TEMP AND IO INTO AVE CALCULATION FOLLOWS
90
11
AREA = PI*(S/2.0)**2
TAVE = T(2,1)*AREA
NOTE 12
BEGIN DO LOOP 300 K = 2, JBARM
13
AREA = AREA + 2.0*PI*R(K)*S
TAVE = TAVE + T(2,K) *2.0*PI*R(K)*S
300
14
END OF DO LOOP?
NO
YES
15
AREAR = PI*(R(K) - S/4.0)*S
TAVE = TAVE + T(2, JBAR)*AREAR
AREA = AREA + AREAR
16
TAVE = TAVE/AREA
UPROP = (U(ITOPM) + TAVE + T(II,1))/3.0 + 460.0
IPROP = IFIX(UPROP/50.0) + 1
17
IPROP .GT. IVAL
FALSE
05.17--->
TRUE
5.19
18
IPROP = IVAL
19
DIFUS = DIF(IPROP)/25.0
M = S**2/(DIFUS*DELT)
TP(II,J) = (U(ITOPM) + TAVE)/M + (1.0 - 2.0/M)*T(II,J)
20
UP(ITOP) = TP(1,1)
8.06.
200

CHART TITLE - PART FOUR

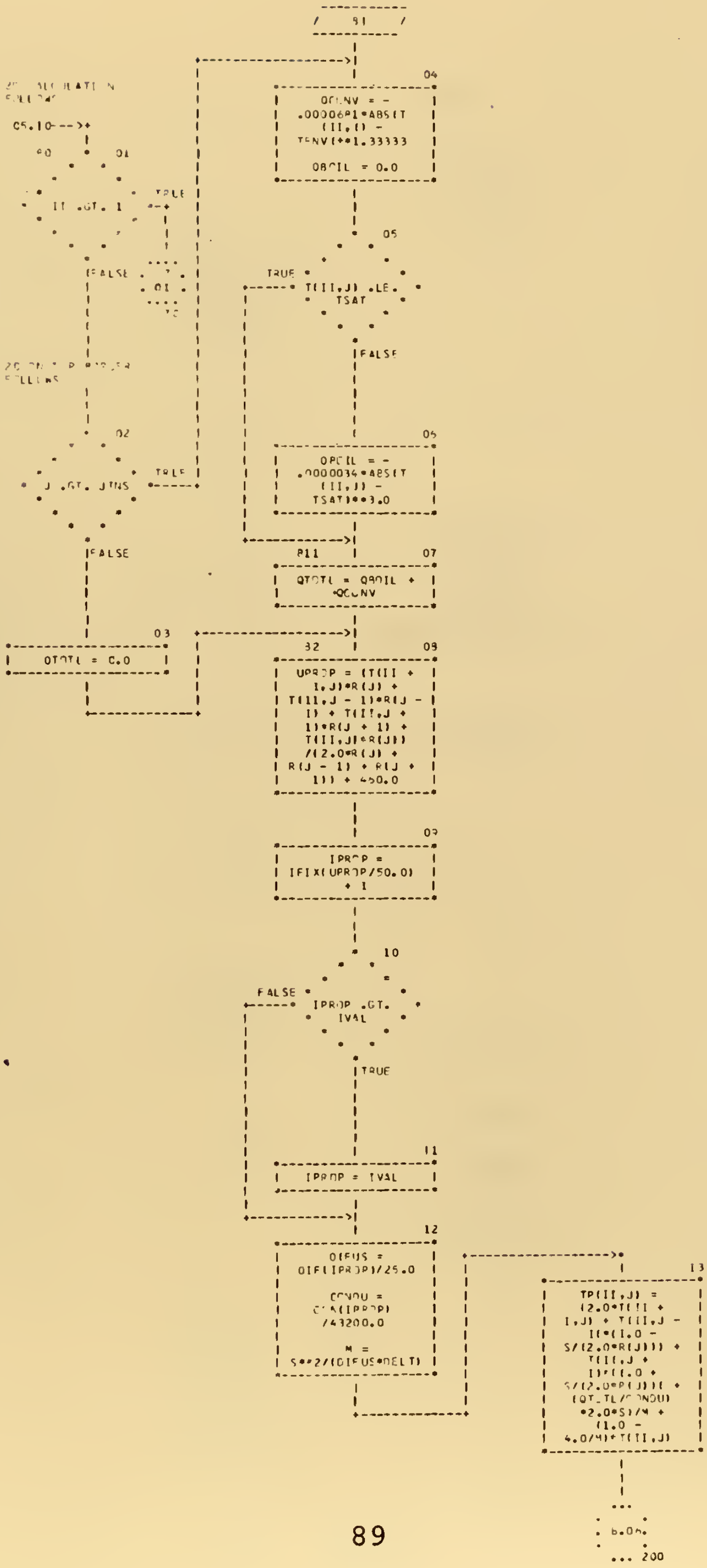

CHART TITLE - PROCEDURES

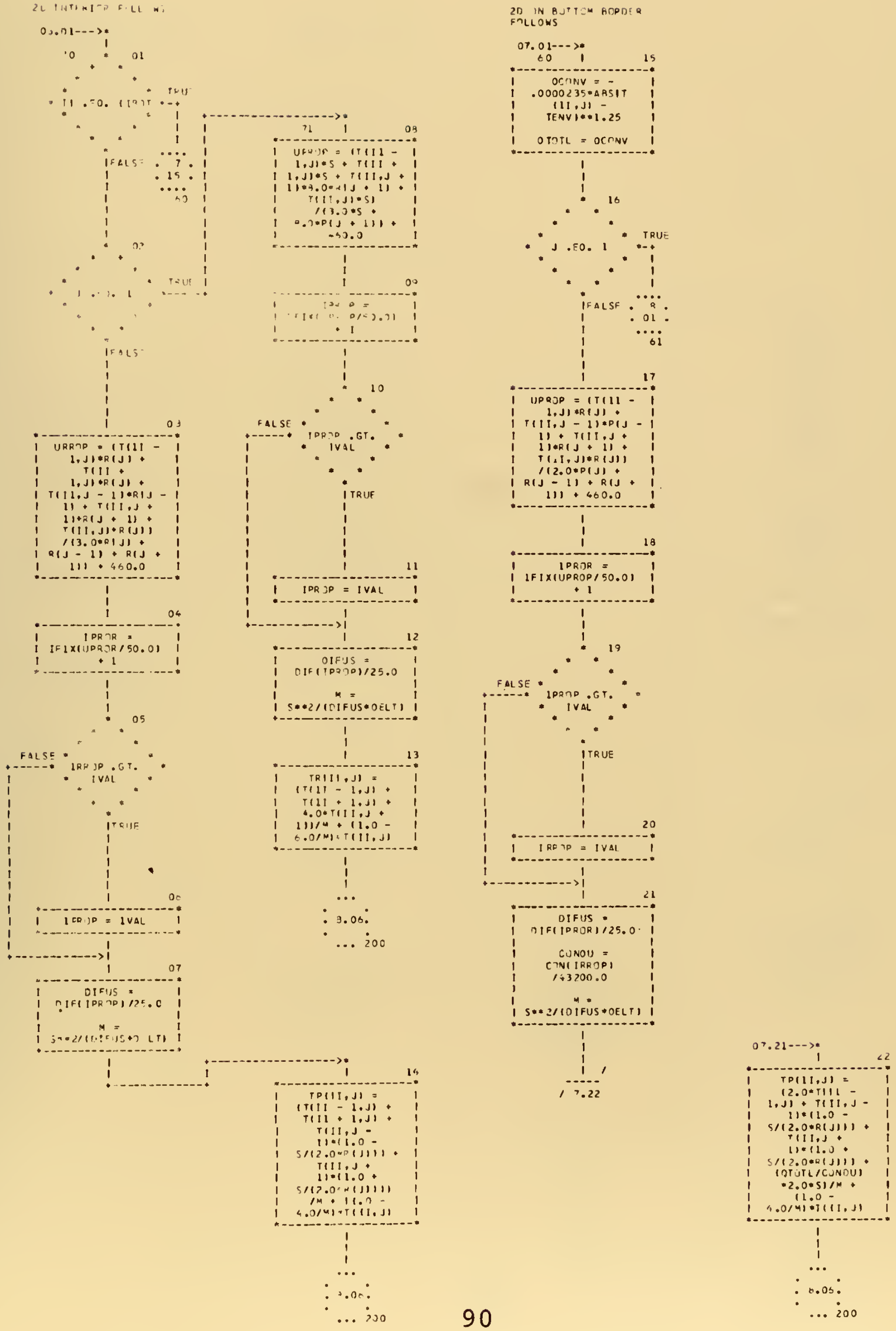

```
01  II .EQ. (IROT
02  J .EQ. 1
03  URROP = (T(II - 1,J)*R(J) + T(II + 1,J)*R(J) + T(II,J - 1)*R(J - 1) + T(II,J + 1)*R(J + 1) + T(II,J)*R(J)) /(3.0*R(J) + R(J - 1) + R(J + 1)) + 460.0
04  IPROR = IFIX(UPROR/50.0) + 1
05  IRROP .GT. IVAL
06  IPROP = IVAL
07  DIFUS = DIF(IPROP)/25.0
    M = S**2/(DIFUS*DELT)
08  UPROP = (T(II - 1,J)*S + T(II + 1,J)*S + T(II,J + 1)*8.0*R(J + 1) + T(II,J)*S) /(3.0*S + 8.0*P(J + 1)) + 460.0
09  IPROP = IFIX(UPROP/50.0) + 1
10  IPROP .GT. IVAL
11  IPROP = IVAL
12  DIFUS = DIF(IPROP)/25.0
    M = S**2/(DIFUS*DELT)
13  TR(II,J) = (T(II - 1,J) + T(II + 1,J) + 4.0*T(II,J + 1))/M + (1.0 - 6.0/M)*T(II,J)
14  TP(II,J) = (T(II - 1,J) + T(II + 1,J) + T(II,J - 1)*(1.0 - S/(2.0*P(J))) + T(II,J + 1)*(1.0 + S/(2.0*R(J)))) /M + (1.0 - 4.0/M)*T(II,J)
15  OCONV = - .0000235*ABS(T(II,J) - TENV)**1.25
    QTOTL = QCONV
16  J .EQ. 1
17  UPROP = (T(II - 1,J)*R(J) + T(II,J - 1)*P(J - 1) + T(II,J + 1)*R(J + 1) + T(II,J)*R(J)) /(2.0*P(J) + R(J - 1) + R(J + 1)) + 460.0
18  IPROR = IFIX(UPROP/50.0) + 1
19  IPROP .GT. IVAL
20  IRPOP = IVAL
21  DIFUS = DIF(IPROR)/25.0
    CONDU = CON(IRROP) /43200.0
    M = S**2/(DIFUS*DELT)
22  TP(II,J) = (2.0*T(II - 1,J) + T(II,J - 1)*(1.0 - S/(2.0*R(J))) + T(II,J + 1)*(1.0 + S/(2.0*R(J))) + (QTOTL/CONDU) *2.0*S)/M + (1.0 - 4.0/M)*T(II,J)
```

CHART TITLE - PROCEDURES

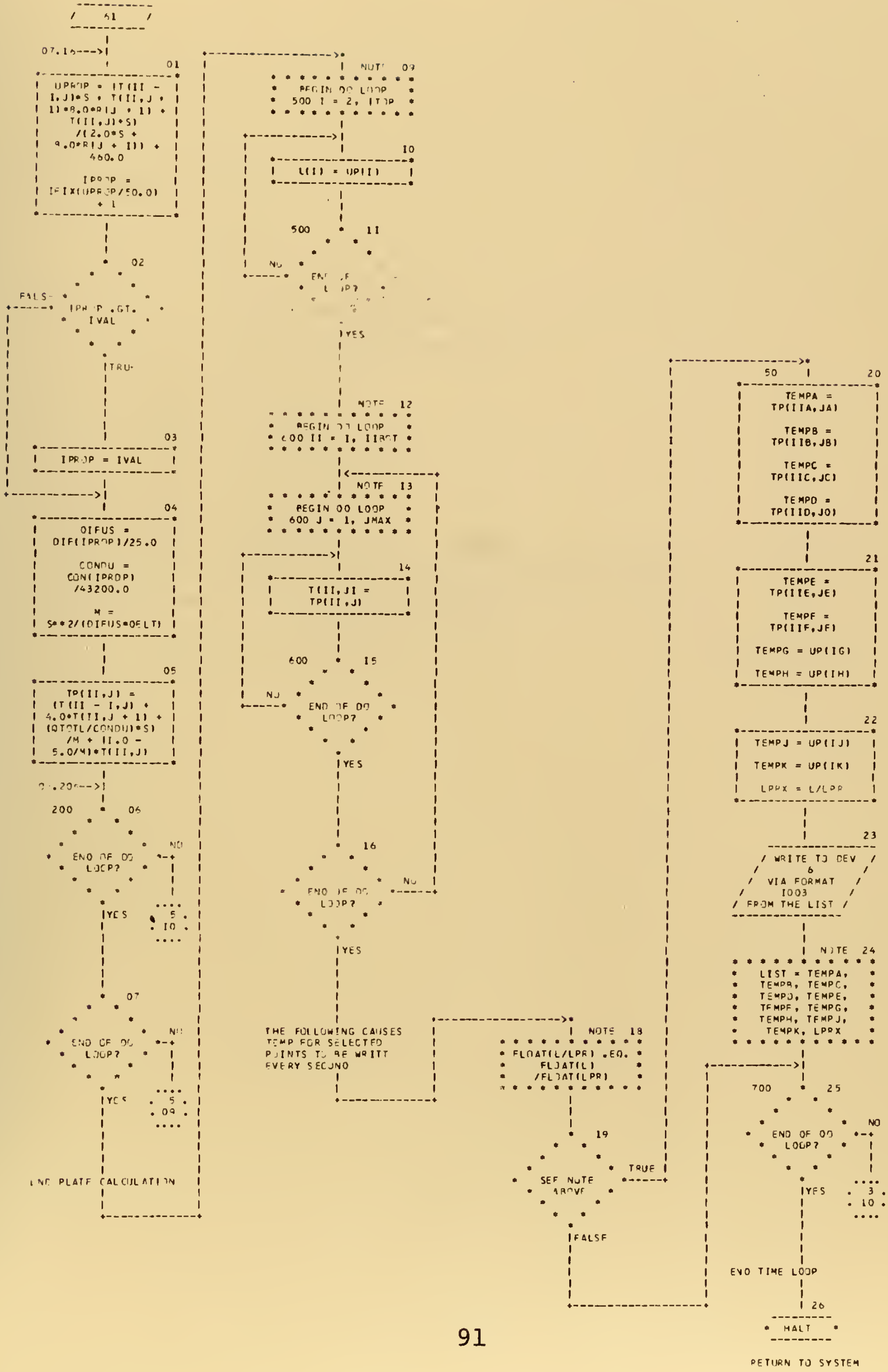

CHART TITLE - NON-PROCEDURAL STATEMENTS

```
               REAL M
               DIMENSION T(21,100),TP(21,100),U(100),JP(100),[illegible]
               ETA(10),TPROP(100),CON(100),DIF(100)
 1006          FORMAT (4F10.-)
 1007          FORMAT (5F10.-)
 1008          FORMAT (2F10.-)
 1004          FORMAT (I3)
 1005          FORMAT (3F10.5)
 1009          FORMAT (2F10.4)
 1010          FORMAT (12I5)
 1011          FORMAT (4I5)
 1000          FORMAT ('1',T20,'TEMPERATURE HISTORIES OF SELECTED POINTS')
 1001          FORMAT ('0',9X,'A',9X,'B',9X,'C',9X,'D',9X,'E',9X,'F',9X,'G',9X,
                       'H',9X,'J',9X,'K',9X,'SEC')
 1003          FORMAT (10X,10F9.0,I10)
```

```
C                PROGRAM FOR PREDICTING TEMPERATURE DISTRIBUTIONS OF BAR TO
C                PLATE THERMIT WELD UNDERWATER
C
C
      REAL M
      DIMENSION T(21,100),TP(21,100),U(100),UP(100),R(100),BETA(10),
     2ETA(10),TPROF(100),CON(100),DIF(100)
      READ(5,1006) TENV,TSAT,TSOL,THERM
 1006 FORMAT (4F10.4)
      READ(5,1007) GAP,RBAR,RINS,THICK,EFF
 1007 FORMAT (5F10.4)
      READ(5,1008) RHO,QFUS
 1008 FORMAT (2F10.4)
      READ (5,1004) IVAL
 1004 FORMAT (I3)
      READ(5,1005) (TPROP(IPROP),CON(IPROP),DIF(IPROP),IPROP=1,IVAL)
 1005 FORMAT (3F10.5)
      READ(5,1009) TSIM,FLOW
 1009 FORMAT (2F10.4)
      READ(5,1010) IIA,JA,IIB,JB,IIC,JC,IID,JD,IIE,JE,IIF,JF
 1010 FORMAT (12I5)
      READ(5,1011) IG,IH,IJ,IK
 1011 FORMAT (4I5)
      WRITE (6,1000)
      WRITE (6,1001)
C
      PI=3.14159
      S=0.125
C                UNITS: IN
      DELT=0.1
C                UNITS: SEC
      EVAC=FLOW*0.5
C                UNITS: SEC
      LEVAC=IFIX(EVAC/DELT)
      LFLOW=IFIX(FLOW/DELT)
      THERM=THERM*EFF
```

```
      THERI=THERM-140.0
      QFUS=-QFUS
      DO 25 IZ=1,10
      BETA(IZ)=999.9
      ETA(IZ)=0.0
   25 CONTINUE
      TEND=TSIM/DELT
      LTEND=IFIX(TEND)
      ITOP=100
      ITOPM=99
      IIBOT=IFIX(THICK/S)+1
      JMAX=49
      JMAXP=50
      JBAR=IFIX(RBAR/S)+1
      JBARM=JBAR-1
      JINS=IFIX(RINS/S)+1
      LPR=IFIX(1.0/DELT)
      R(1)=0.0
      DO 10   J=2,JMAXP
      R(J)=R(J-1)+S
   10 CONTINUE
      DO 20   I=1,ITOP
      U(I)=TENV
      UP(I)=TENV
   20 CONTINUE
      DO 30   II=1,IIBOT
      DO 30   J=1,JMAXP
      T(II,J)=TENV
      TP(II,J)=TENV
   30 CONTINUE
      IGAP=ITOP-IFIX(GAP/S)
      DO 40   I=IGAP,ITOPM
      U(I)=THERM
   40 CONTINUE
      IIA=IIA+1
      JA=JA+1
```

```
      IIB=IIB+1
      JB=JB+1
      IIC=IIC+1
      JC=JC+1
      IID=IID+1
      JD=JD+1
      IIF=IIE+1
      JE=JE+1
      IIF=IIF+1
      JF=JF+1
      IG=100-IG
      IH=100-IH
      IJ=100-IJ
      IK=100-IK
C
C                START TIME LOOP
C
      DO 700  L=1,LTEND
C
C                BAR TEMP CALCULATION FOLLOWS
C
      DO 100 I=50,ITOP4
      IY=I-IGAP+1
  991 UPROP=(U(I-1)+U(I+1)+U(I))/3.0+460.0
      IPROP=IFIX(UPROP/50.0)+1
      IF(IPROP.GT.IVAL) IPROP=IVAL
      DIFUS=DIF(IPROP)/25.0
      CONDU=CON(IPROP)/43200.0
      M=S**2/(DIFUS*DELT)
      UP(I)=(U(I-1)+U(I+1))/M+(1.0-2.0/M)*U(I)
      IF(I.LT.IGAP) GO TO 100
  992 IF(L.GT.LEVAC) GO TO 991
      DO 98 IX=IGAP, ITOP4
      UP(IX)=THERI
   98 CONTINUE
      GO TO 100
```

```
  991 IF(L.GT.LFLOW) GO TO 997
      DO 99 IW=IGAP,ITOPM
      UP(IW)=THERM
   99 CONTINUE
      GO TO 100
C
C                START SOLIDIFICATION ROUTINE
C
  997 IF(U(I).GE.TSOL.AND.UP(I).LE.TSOL) GO TO 992
      GO TO 100
  992 IF(BETA(IY).EQ.999.9) GO TO 996
      IF(BETA(IY).LT.(1.0-ETA(IY))) GO TO 994
      GO TO 995
  996 UP(I)=TSOL
      ETA(IY)=(U(I-1)+U(I+1)-2.0*U(I)-M*(TSOL-U(I)))*CONDU*DELT
     2/(RHO*QFUS*S**2)
      IF(ETA(IY).LT.1.0) GO TO 99
      IF(ETA(IY).EQ.1.0) GO TO 100
  995 UP(I)=(U(I-1)+U(I+1)-(RHO*QFUS*S**2)/CONDU)/M+(1.0-2.0/M)*U(I)
      ETA(IY)=0.0
      GO TO 100
  994 ETA(IY)=ETA(IY)+BETA(IY)
  993 BETA(IY)=(U(I-1)+U(I+1)-2.0*U(I))*DELT*CONDU/(RHO*QFUS*S**2)
  100 CONTINUE
C
C                END BAR TEMPERATURE CALCULATION
C
      DO 200  II=1,IIBOT
      DO 200  J=1,JMAX
      IF(II.EQ.1.AND.J.LE.JBAR) GO TO 90
      GO TO 80
C
C                AVE TEMP AND ID INTO AVE CALCULATION FOLLOWS
C
   90 AREA=PI*(S/2.0)**2
      TAVE=T(2,1)*AREA
```

```
      DO 300  K=2,JBARM
      AREA=AREA+2.0*PI*R(K)*S
      TAVE=TAVE+T(2,K)*2.0*PI*R(K)*S
  300 CONTINUE
      AREAR=PI*(R(K)-S/4.0)*S
      TAVE=TAVE+T(2,JBAR)*AREAR
       AREA=AREA+AREAR
      TAVE=TAVE/AREA
      UPROP=(U(ITOP4)+TAVE+T(II,J))/3.0+460.0
      IPROP=IFIX(UPROP/50.0)+1
      IF(IPROP.GT.IVAL) IPROP=IVAL
      DIFUS=DIF(IPROP)/25.0
      M=S**2/(DIFUS*DELT)
      TP(II,J)=(U(ITOP4)+TAVE)/M+(1.0-2.0/M)*T(II,J)
      UP(ITOP)=TP(1,1)
      GO TO 200
C
C                 2D CALCULATION FOLLOWS
C
   80 IF(II.GT.1) GO TO 70
C
C                 2D ON TOP BORDER FOLLOWS
C
       IF(J.GT.JINS)GO TO 81
      QTOTL=0.0
      GO TO 82
   81 QCONV=-.0000681*ABS(T(II,J)-TENV)**1.33333
       QBOIL=0.0
      IF(T(II,J).LE.TSAT) GO TO 811
      QBOIL=-.0000034*ABS(T(II,J)-TSAT)**3.0
  811 QTOTL=QBOIL+QCONV
   82 UPROP=(T(II+1,J)*R(J)+T(II,J-1)*R(J-1)+T(II,J+1)*R(J+1)+T(II,J)
     2*R(J))/(2.0*R(J)+R(J-1)+R(J+1))+460.0
      IPROP=IFIX(UPROP/50.0)+1
      IF(IPROP.GT.IVAL) IPROP=IVAL
      DIFUS=DIF(IPROP)/25.0
```

```
      CONDU=CON(IPROP)/43200.0
      M=S**2/(DIFUS*DELT)
      TP(II,J)=(2.0*T(II+1,J)+T(II,J-1)*(1.0-S/(2.0*R(J)))+T(II,J+1)
     2*(1.0+S/(2.0*R(J)))+(QTOTL/CONDU)*2.0*S)/M+(1.0-4.0/M)*T(II,J)
      GO TO 200
C
C                2D INTERIOR FOLLOWS
C
   70 IF(II.EQ.IIBOT) GO TO 60
      IF(J.EQ.1) GO TO 71
      UPROP=(T(II-1,J)*R(J)+T(II+1,J)*R(J)+T(II,J-1)*R(J-1)+T(II,J+1)
     2*R(J+1)+T(II,J)*R(J))/(3.0*R(J)+R(J-1)+R(J+1))+460.0
      IPROP=IFIX(UPROP/50.0)+1
      IF(IPROP.GT.IVAL) IPROP=IVAL
      DIFUS=DIF(IPROP)/25.0
      M=S**2/(DIFUS*DELT)
       TP(II,J)=(T(II-1,J)+T(II+1,J)+T(II,J-1)*(1.0-S/(2.0*R(J)))
     2+T(II,J+1)*(1.0+S/(2.0*R(J))))/M+(1.0-4.0/M)*T(II,J)
      GO TO 200
   71 UPROP=(T(II-1,J)*S+T(II+1,J)*S+T(II,J+1)*8.0*R(J+1)+T(II,J)*S).
     2/(3.0*S+8.0*R(J+1))+460.0
      IPROP=IFIX(UPROP/50.0)+1
      IF(IPROP.GT.IVAL) IPROP=IVAL
      DIFUS=DIF(IPROP)/25.0
      M=S**2/(DIFUS*DELT)
      TP(II,J)=(T(II-1,J)+T(II+1,J)+4.0*T(II,J+1))/M+(1.0-6.0/M)*T(II,J)
      GO TO 200
C
C                2D ON BOTTOM BORDER FOLLOWS
C
   60 QCONV=-.0000235*ABS(T(II,J)-TENV)**1.25
      QTOTL=QCONV
      IF(J.EQ.1) GO TO 61
      UPROP=(T(II-1,J)*R(J)+T(II,J-1)*R(J-1)+T(II,J+1)*R(J+1)+T(II,J)
     2*R(J))/(2.0*R(J)+R(J-1)+R(J+1))+460.0
      IPROP=IFIX(UPROP/50.0)+1
```

```
      IF(IPROP.GT.IVAL) IPROP=IVAL
      DIFUS=DIF(IPROP)/25.0
      CONDU=CON(IPROP)/43200.0
      M=S**2/(DIFUS*DELT)
      TP(II,J)=(2.0*T(II-1,J)+T(II,J-1)*(1.0-S/(2.0*R(J)))+T(II,J+1)
     2*(1.0+S/(2.0*R(J)))+(QTOTL/CONDU)*2.0*S)/M+(1.0-4.0/M)*T(II,J)
      GO TO 200
   61 UPROP=(T(II-1,J)*S+T(II,J+1)*8.0*R(J+1)+T(II,J)*S)/(2.0*S
     2+8.0*R(J+1))+460.0
      IPROP=IFIX(UPROP/50.0)+1
      IF(IPROP.GT.IVAL) IPROP=IVAL
      DIFUS=DIF(IPROP)/25.0
      CONDU=CON(IPROP)/43200.0
      M=S**2/(DIFUS*DELT)
      TP(II,J)=(T(II-1,J)+4.0*T(II,J+1)+(QTOTL/CONDU)*S)/M+(1.0-5.0/M)
     2*T(II,J)
  200 CONTINUE
C
C                END PLATE CALCULATION
C
      DO 500  I=2,ITOP
      U(I)=UP(I)
  500 CONTINUE
      DO 600  II=1,IIBOT
      DO 600  J=1,JMAX
      T(II,J)=TP(II,J)
  600 CONTINUE
C
C                THE FOLLOWING CAUSES TEMP FOR SELECTED POINTS TO BE WRITTEN
C                EVERY SECOND
C
      IF(FLOAT(L/LPR).EQ.FLOAT(L)/FLOAT(LPR)) GO TO 50
      GO TO 700
   50 TEMPA=TP(IIA,JA)
      TEMPB=TP(IIB,JB)
      TEMPC=TP(IIC,JC)
```

```
      TEMPD=TP(IID,JD)
      TEMPE=TP(IIE,JE)
      TEMPF=TP(IIF,JF)
      TEMPG=UP(IG)
      TEMPH=UP(IH)
      TEMPJ=UP(IJ)
      TEMPK=UP(IK)
      LPRX=L/LPR
      WRITE (6,1003) TEMPA, TEMPB, TEMPC, TEMPD, TEMPE, TEMPF, TEMPG,
     2TEMPH, TEMPJ, TEMPK, LPRX
  700 CONTINUE
C
C                   END TIME LOOP
C
 1000 FORMAT ('1',T20,'TEMPERATURE HISTORIES OF SELECTED POINTS')
 1001 FORMAT ('0',9X,'A',9X,'B',9X,'C',9X,'D',9X,'E',9X,'F',9X,'G',9X,
     2        'H',9X,'J',9X,'K',9X,'SEC')
 1003 FORMAT (10X,10F9.0,I10)
      STOP
      END
```

```
C         SAMPLE DATA DECK
C
C
$ENTRY
   40.        212.       2740.       5590.
    0.5         0.5         1.0         1.0         0.68
    0.2835 1213.38
  70
   50.         45.5        2.31225
  100.         44.5        2.05584
  150.         43.5        1.57996
  200.         42.5        1.30599
  250.         41.3        1.12003
  300.         41.         1.04429
  350.         40.          .99457
  400.         39.2         .89311
  450.         38.5         .82756
  500.         37.6         .76945
  550.         36.3         .73789
  600.         36.1         .70351
  650.         35.2         .65597
  700.         34.5         .61482
  750.         33.3         .58294
  800.         32.8         .56193
  850.         32.          .54489
  900.         31.2         .52739
  950.         30.5         .50348
 1000.         29.7         .47912
 1050.         29.          .44432
 1100.         28.2         .41701
 1150.         27.5         .40462
 1200.         26.8         .39177
 1250.         25.9         .35928
 1300.         25.          .33571
 1350.         24.5         .31919
 1400.         23.3         .29566
```

1450.	23.1	.27598
1500.	22.2	.24465
1550.	21.8	.22843
1600.	21.1	.20136
1650.	20.6	.14922
1700.	20.	.14046
1750.	19.5	.12877
1800.	19.	.13334
1850.	18.8	.1523
1900.	18.1	.18214
1950.	17.9	.2351
2000.	17.2	.22717
2050.	17.	.22453
2100.	16.5	.21793
2150.	16.1	.21264
2200.	15.9	.21
2250.	15.5	.20583
2300.	15.2	.20165
2350.	15.	.19935
2400.	14.9	.19855
2450.	14.5	.19379
2500.	14.1	.18895
2550.	14.0	.184
2600.	13.7	.1805
2650.	13.4	.177
2700.	13.2	.1735
2750.	12.9	.17
2800.	12.6	.166
2850.	12.4	.163
2900.	12.1	.159
2950.	11.8	.1555
3000.	11.5	.152
3050.	11.3	.148
3100.	11.0	.145
3150.	10.7	.141
3200.	10.5	.138

```
3250.        10.2       .134
3300.         9.9       .131
3350.         9.7       .127
3400.         9.4       .124
3450.         9.1       .120
3500.         8.9       .116
  120.         1.0
    4    16    6    8    4.   4    2    0    1    4    1    8
    50    3    2    1
```

TEMPERATURE HISTORIES OF SELECTED POINTS

A	B	C	D	E	F	G	H	J	K	SEC
40.	40.	44.	157.	363.	41.	40.	3801.	3801.	3901.	1
40.	40.	85.	419.	717.	59.	40.	3735.	3734.	3280.	2
40.	43.	146.	618.	912.	89.	40.	3597.	3597.	3040.	3
40.	50.	207.	753.	1023.	123.	40.	3449.	3448.	2896.	4
40.	60.	262.	846.	1092.	154.	40.	3308.	3305.	2791.	5
40.	72.	308.	921.	1138.	182.	40.	3178.	3174.	2710.	6
41.	87.	349.	982.	1167.	207.	40.	3059.	3052.	2626.	7
42.	101.	385.	1028.	1190.	228.	40.	2945.	2935.	2549.	8
43.	116.	416.	1065.	1206.	248.	40.	2840.	2825.	2475.	9
44.	131.	444.	1092.	1216.	265.	40.	2742.	2728.	2404.	10
46.	145.	468.	1111.	1220.	280.	40.	2657.	2631.	2336.	11
48.	159.	489.	1124.	1220.	294.	40.	2571.	2541.	2270.	12
50.	172.	508.	1133.	1217.	306.	40.	2491.	2457.	2207.	13
53.	185.	524.	1137.	1210.	317.	40.	2416.	2379.	2145.	14
55.	196.	538.	1138.	1202.	327.	40.	2346.	2306.	2087.	15
58.	208.	550.	1137.	1191.	335.	40.	2280.	2237.	2030.	16
61.	218.	560.	1133.	1179.	341.	40.	2217.	2172.	1976.	17
64.	228.	569.	1128.	1166.	347.	40.	2159.	2111.	1924.	18
66.	237.	576.	1121.	1150.	351.	40.	2103.	2053.	1876.	19
69.	246.	582.	1113.	1135.	355.	40.	2050.	1999.	1829.	20
72.	253.	587.	1104.	1119.	358.	40.	2000.	1947.	1784.	21
75.	261.	590.	1093.	1103.	360.	40.	1952.	1898.	1741.	22
78.	267.	593.	1082.	1086.	362.	40.	1907.	1852.	1700.	23
80.	273.	594.	1070.	1070.	364.	40.	1865.	1808.	1662.	24
83.	278.	595.	1057.	1055.	365.	40.	1825.	1767.	1625.	25
86.	283.	595.	1044.	1040.	366.	40.	1786.	1728.	1591.	26
88.	288.	595.	1031.	1026.	366.	40.	1749.	1691.	1559.	27
90.	292.	593.	1018.	1012.	366.	40.	1714.	1656.	1529.	28
93.	295.	592.	1005.	998.	366.	40.	1681.	1622.	1499.	29
95.	298.	590.	991.	984.	366.	40.	1649.	1590.	1471.	30
97.	301.	588.	977.	971.	365.	40.	1618.	1560.	1446.	31
99.	303.	585.	963.	957.	365.	40.	1589.	1532.	1423.	32
101.	305.	582.	950.	944.	364.	40.	1562.	1506.	1401.	33
103.	307.	579.	937.	931.	363.	40.	1535.	1480.	1380.	34
105.	308.	576.	924.	919.	362.	40.	1511.	1456.	1359.	35
107.	310.	572.	912.	906.	361.	40.	1488.	1437.	1339.	36
109.	311.	568.	900.	893.	360.	40.	1466.	1417.	1320.	37
110.	311.	564.	888.	881.	359.	40.	1447.	1398.	1302.	38
112.	312.	560.	876.	869.	357.	40.	1431.	1381.	1283.	39
113.	312.	556.	864.	857.	356.	40.	1416.	1364.	1265.	40

115.	312.	552.	852.	846.	354.	40.	1400.	1348.	1247.	41
116.	312.	548.	841.	834.	353.	40.	1387.	1333.	1230.	42
117.	312.	543.	830.	824.	351.	40.	1374.	1318.	1213.	43
118.	312.	539.	819.	813.	349.	40.	1361.	1303.	1197.	44
120.	311.	534.	809.	803.	348.	40.	1348.	1289.	1182.	45
121.	311.	530.	799.	793.	346.	40.	1336.	1275.	1167.	46
122.	310.	525.	789.	784.	344.	40.	1324.	1261.	1153.	47
123.	309.	521.	779.	774.	343.	40.	1312.	1247.	1136.	48
123.	308.	516.	770.	765.	341.	40.	1300.	1232.	1120.	49
124.	307.	512.	761.	756.	339.	40.	1288.	1218.	1106.	50
125.	306.	508.	752.	747.	337.	40.	1276.	1205.	1092.	51
126.	305.	503.	743.	738.	336.	40.	1265.	1191.	1078.	52
127.	304.	499.	734.	730.	334.	40.	1253.	1178.	1065.	53
127.	303.	494.	725.	721.	332.	40.	1240.	1165.	1052.	54
128.	302.	490.	717.	713.	330.	40.	1228.	1152.	1040.	55
128.	301.	486.	709.	705.	328.	40.	1216.	1137.	1027.	56
129.	299.	482.	701.	698.	327.	41.	1204.	1123.	1015.	57
129.	298.	477.	693.	690.	325.	41.	1192.	1111.	1003.	58
130.	297.	473.	686.	682.	323.	41.	1179.	1098.	990.	59
130.	295.	469.	678.	675.	321.	41.	1167.	1085.	979.	60
130.	294.	465.	671.	668.	320.	41.	1155.	1072.	967.	61
131.	292.	461.	664.	661.	318.	41.	1141.	1060.	956.	62
131.	291.	457.	656.	654.	316.	41.	1128.	1048.	944.	63
131.	289.	453.	649.	647.	314.	41.	1116.	1035.	933.	64
131.	288.	449.	642.	640.	313.	41.	1103.	1023.	922.	65
132.	286.	446.	636.	633.	311.	41.	1091.	1011.	911.	66
132.	285.	442.	629.	626.	309.	41.	1078.	1000.	901.	67
132.	283.	438.	622.	620.	307.	41.	1066.	988.	890.	68
132.	282.	434.	616.	613.	306.	41.	1054.	976.	879.	69
132.	280.	430.	609.	607.	304.	41.	1041.	964.	869.	70
132.	279.	427.	603.	601.	302.	41.	1029.	953.	859.	71
132.	277.	423.	596.	594.	300.	41.	1016.	941.	849.	72
132.	276.	420.	590.	588.	299.	42.	1004.	930.	839.	73
132.	274.	416.	584.	582.	297.	42.	992.	919.	828.	74
132.	273.	412.	578.	576.	295.	42.	980.	907.	819.	75
132.	271.	409.	572.	570.	294.	42.	968.	896.	809.	76
132.	270.	405.	566.	564.	292.	42.	957.	885.	799.	77
132.	268.	402.	560.	559.	290.	42.	945.	875.	790.	78
132.	267.	398.	554.	552.	288.	42.	934.	864.	780.	79
132.	265.	395.	548.	546.	287.	42.	922.	854.	771.	80

132.	264.	392.	542.	540.	285.	42.	911.	843.	762.	81
132.	262.	383.	536.	535.	283.	42.	901.	833.	753.	82
132.	260.	385.	531.	529.	282.	42.	890.	823.	744.	83
132.	259.	382.	525.	523.	280.	43.	879.	813.	735.	84
131.	257.	378.	520.	518.	278.	43.	869.	804.	726.	85
131.	256.	375.	514.	513.	276.	43.	859.	794.	718.	86
131.	254.	372.	509.	507.	275.	43.	849.	785.	709.	87
131.	253.	369.	504.	502.	273.	43.	839.	775.	701.	88
131.	251.	365.	498.	497.	271.	43.	829.	766.	693.	89
130.	250.	362.	493.	492.	270.	43.	819.	757.	685.	90
130.	248.	359.	488.	487.	268.	43.	810.	749.	677.	91
130.	247.	356.	483.	482.	266.	43.	801.	740.	669.	92
130.	245.	353.	478.	477.	264.	43.	791.	731.	662.	93
130.	244.	350.	473.	472.	263.	44.	782.	723.	654.	94
129.	242.	347.	468.	467.	261.	44.	773.	715.	647.	95
129.	241.	344.	464.	462.	259.	44.	765.	706.	640.	96
129.	239.	341.	459.	458.	257.	44.	756.	699.	632.	97
128.	238.	338.	454.	453.	256.	44.	748.	691.	626.	98
128.	236.	335.	450.	449.	254.	44.	739.	683.	619.	99
128.	235.	333.	445.	444.	252.	44.	731.	675.	612.	100
128.	233.	330.	441.	440.	250.	44.	723.	668.	605.	101
127.	232.	327.	436.	435.	249.	44.	715.	661.	599.	102
127.	230.	324.	432.	431.	247.	44.	707.	654.	592.	103
127.	229.	321.	428.	427.	245.	45.	700.	647.	586.	104
126.	227.	319.	424.	423.	243.	45.	692.	640.	580.	105
126.	226.	316.	420.	419.	242.	45.	685.	633.	573.	106
125.	224.	313.	415.	415.	240.	45.	678.	626.	567.	107
125.	223.	311.	411.	411.	238.	45.	671.	619.	561.	108
125.	221.	308.	408.	407.	237.	45.	664.	613.	556.	109
124.	220.	306.	404.	403.	235.	45.	657.	607.	550.	110
124.	218.	303.	400.	399.	233.	45.	650.	600.	544.	111
124.	217.	301.	396.	395.	232.	45.	643.	594.	539.	112
123.	216.	298.	392.	391.	230.	46.	637.	588.	533.	113
123.	214.	296.	389.	388.	228.	46.	630.	582.	528.	114
122.	213.	293.	385.	384.	227.	46.	624.	576.	522.	115
122.	211.	291.	381.	381.	225.	46.	618.	570.	517.	116
122.	210.	288.	378.	377.	223.	46.	612.	564.	512.	117
121.	208.	286.	374.	374.	222.	46.	606.	559.	507.	118
121.	207.	284.	371.	370.	220.	46.	600.	553.	502.	119
120.	206.	281.	367.	367.	219.	46.	594.	548.	497.	120

APPENDIX E

TEMPERATURE HISTORY DATA TAPES

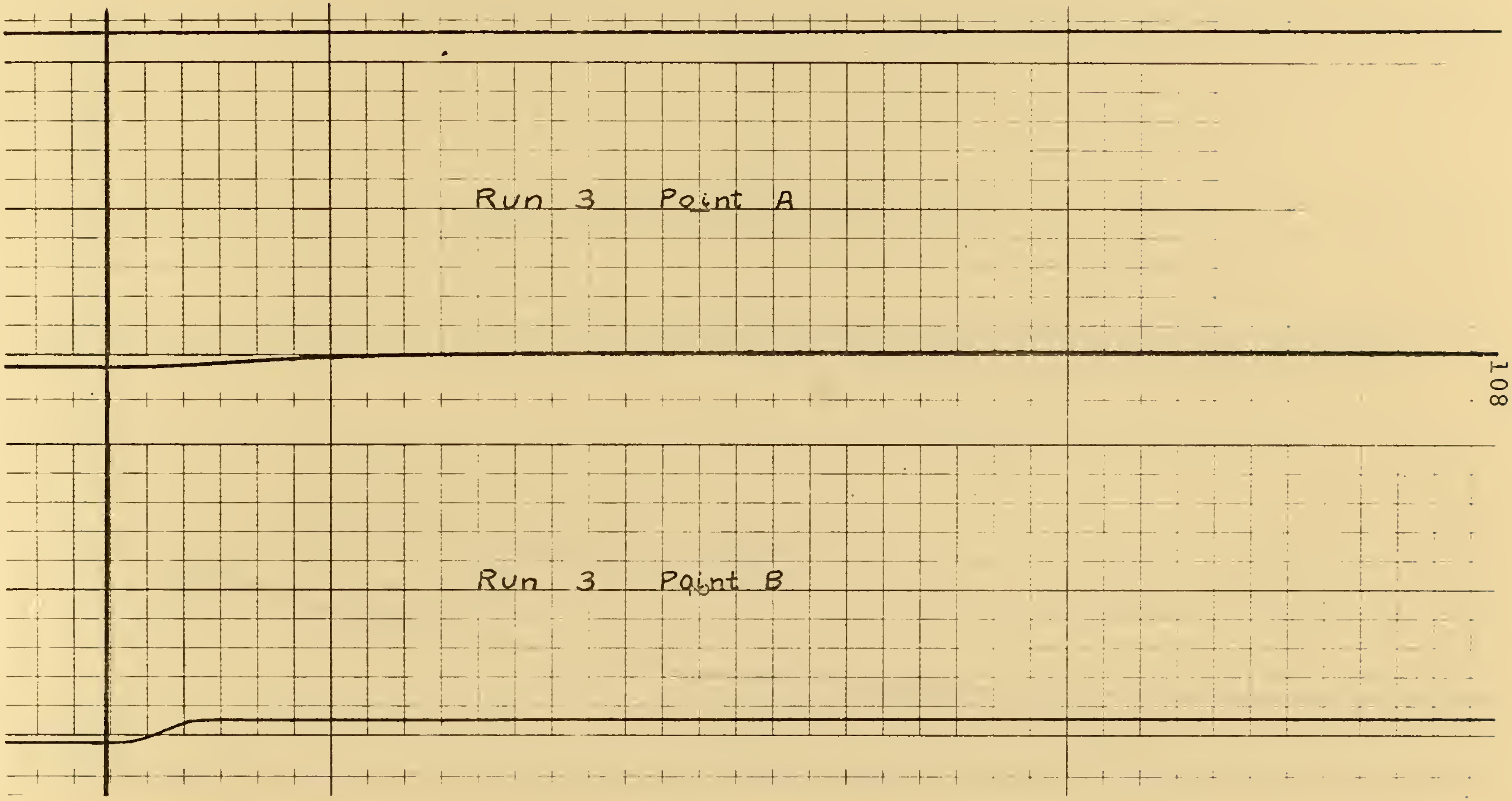
Run 3 Point A
Run 3 Point B

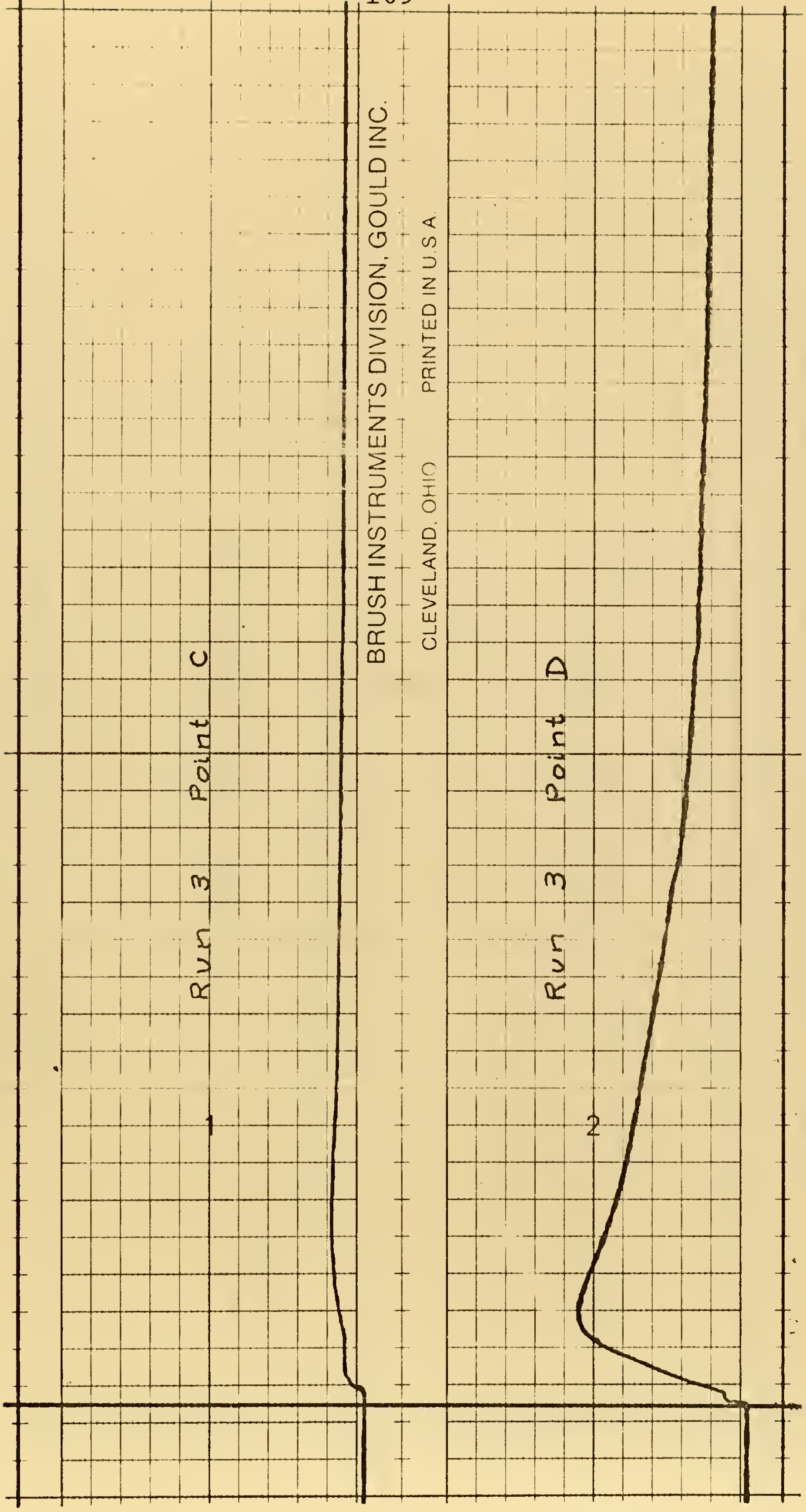
BRUSH INSTRUMENTS DIVISION, GOULD INC.
CLEVELAND, OHIO
PRINTED IN U.S.A.
Run 3 Point C
Run 3 Point D
1
2

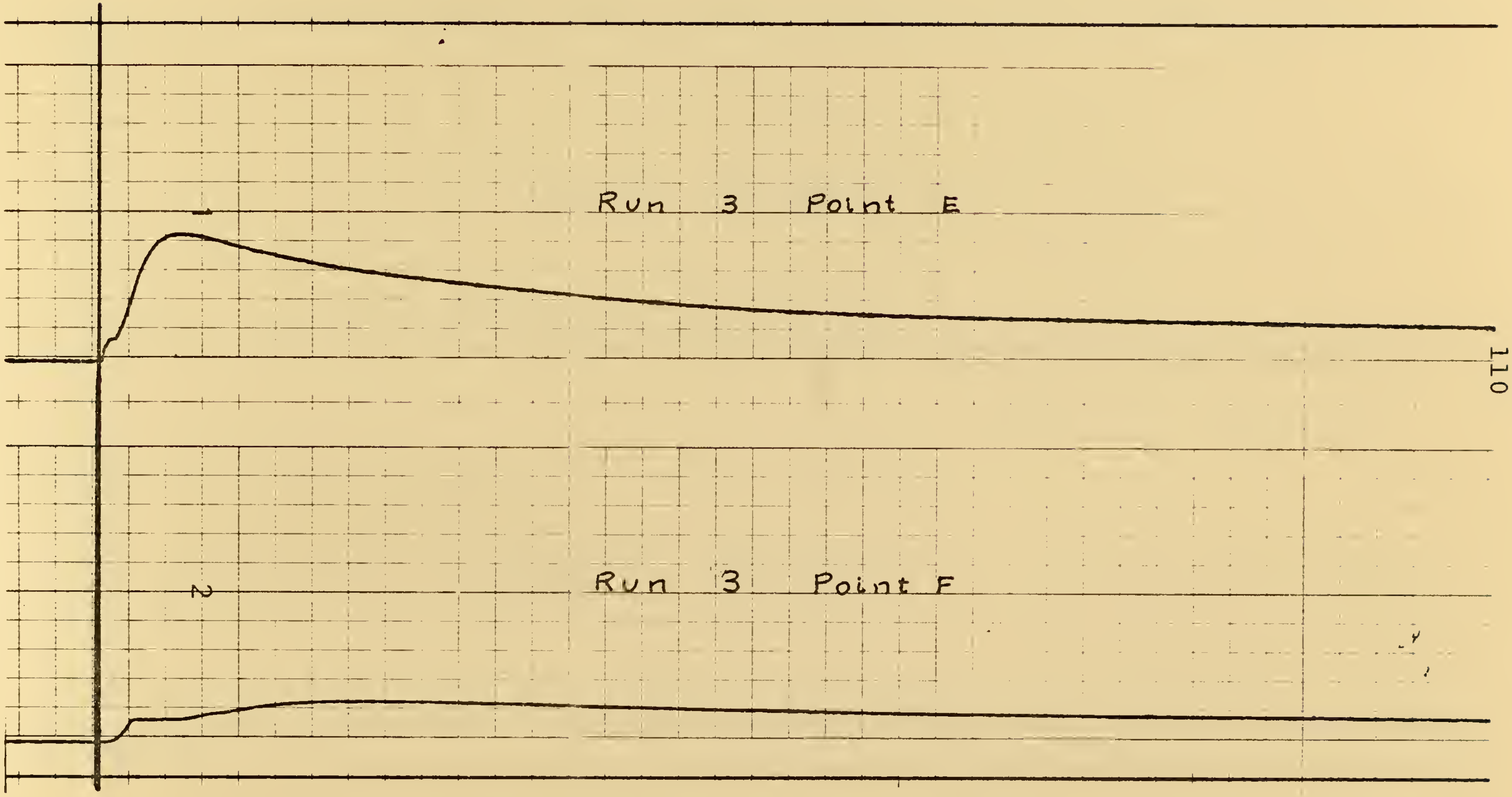
Run 3 Point E
1
Run 3 Point F
2

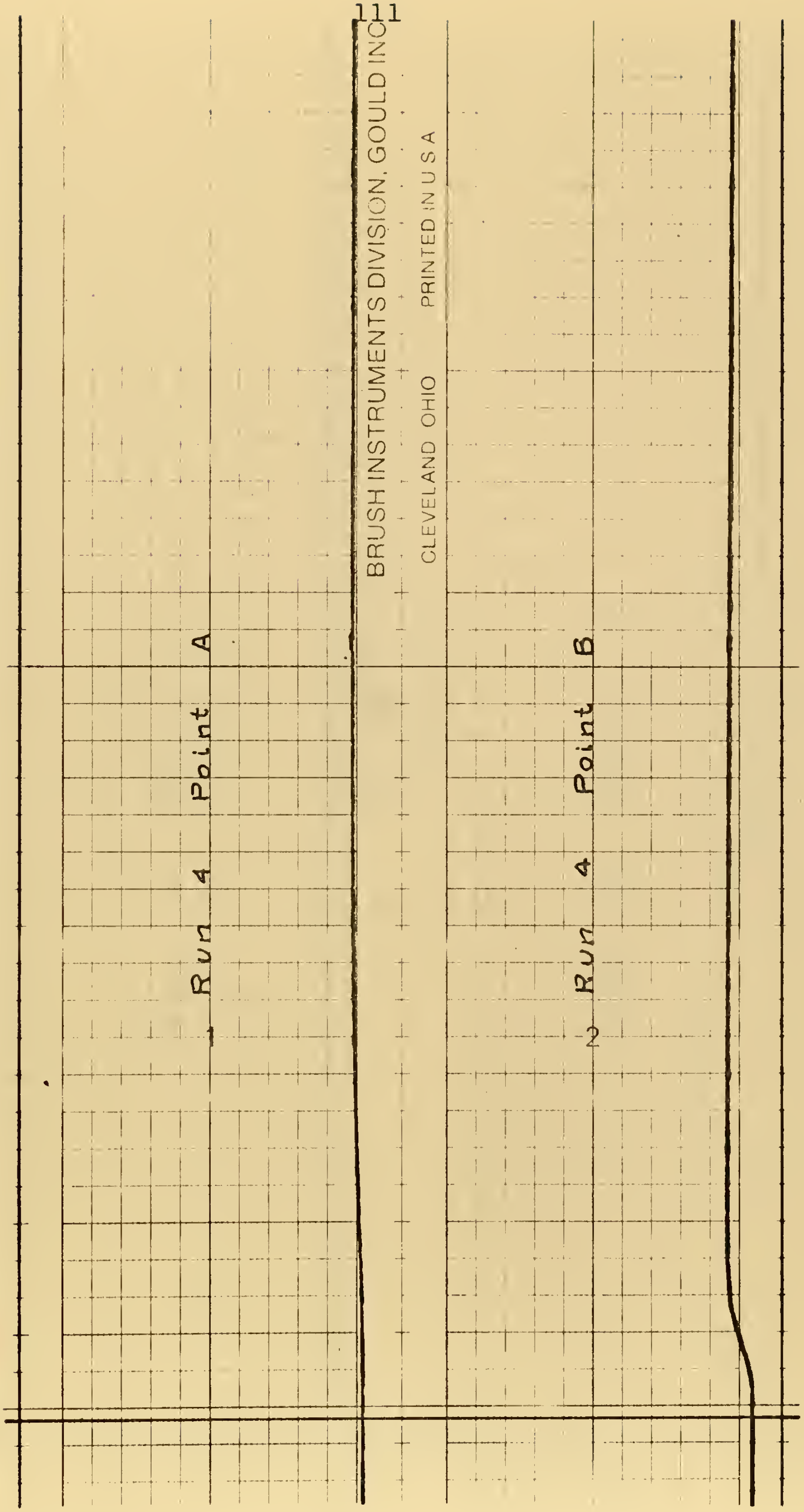
BRUSH INSTRUMENTS DIVISION, GOULD INC.
CLEVELAND OHIO
PRINTED IN U S A
Run 4 Point A
Run 4 Point B
1
2

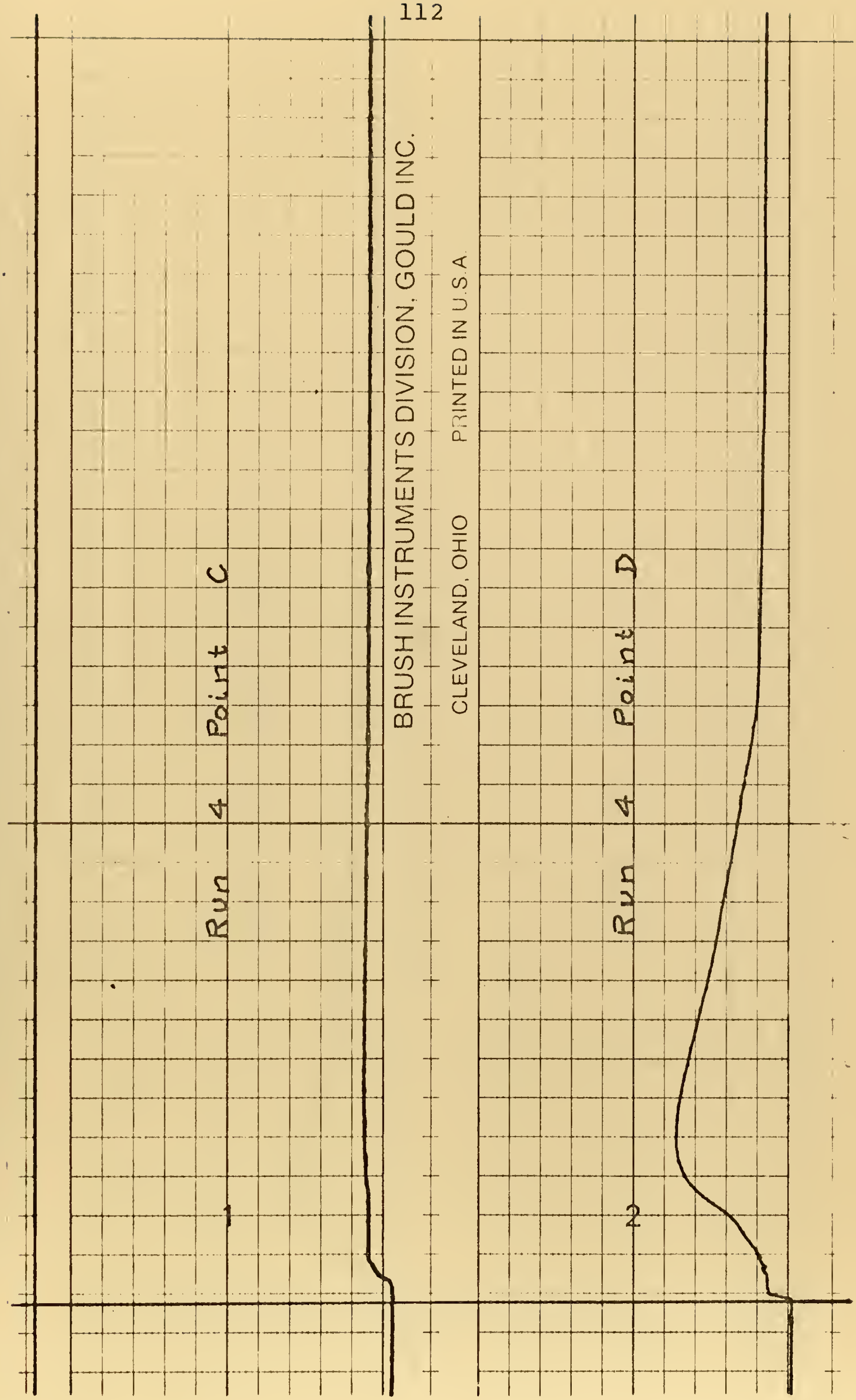
Run 4 Point C
1
BRUSH INSTRUMENTS DIVISION, GOULD INC.
CLEVELAND, OHIO
PRINTED IN U.S.A.
Run 4 Point D
2

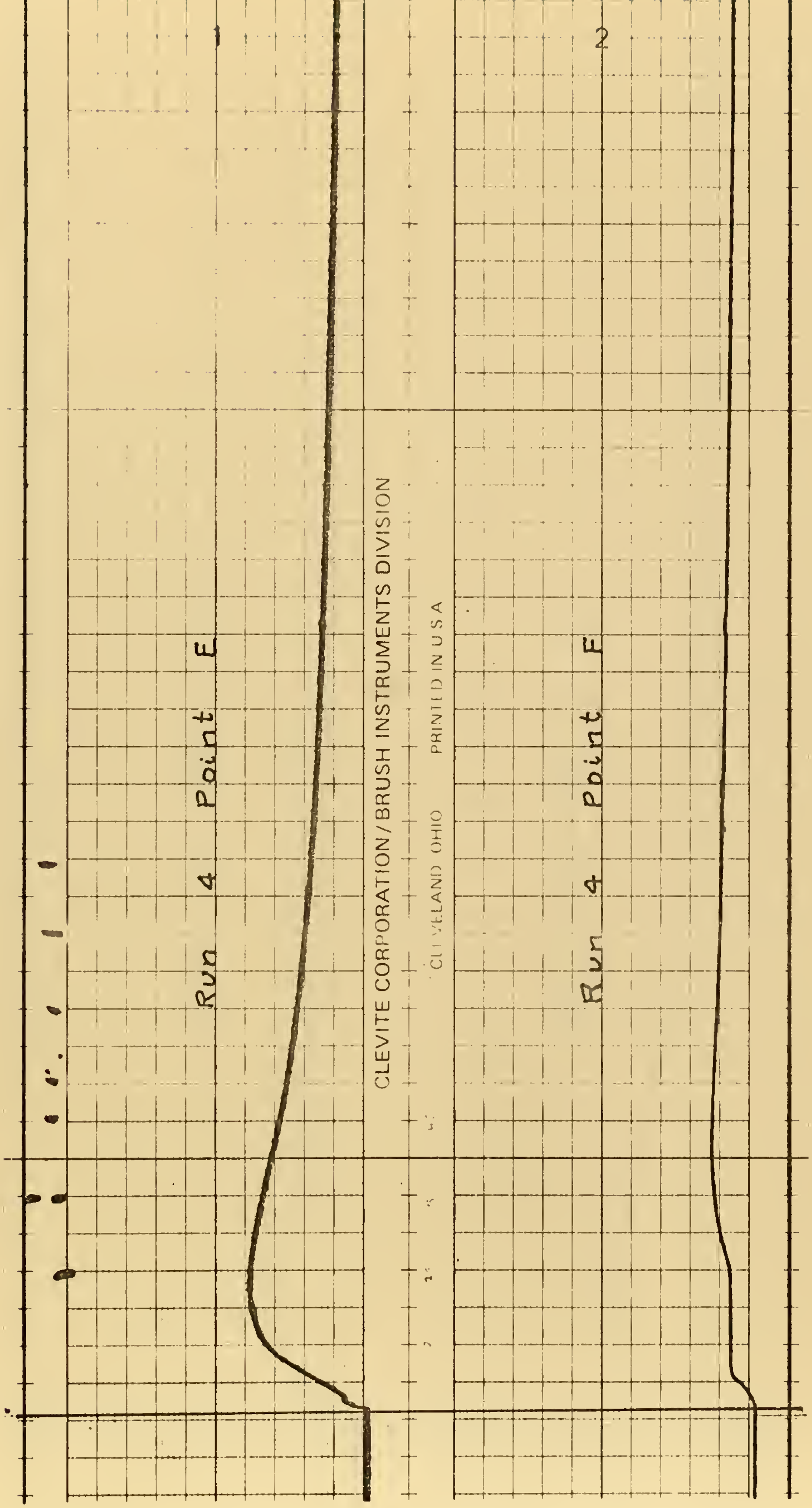
1
2
Run 4 Point E
Run 4 Point F
CLEVITE CORPORATION / BRUSH INSTRUMENTS DIVISION
CLEVELAND OHIO
PRINTED IN U.S.A

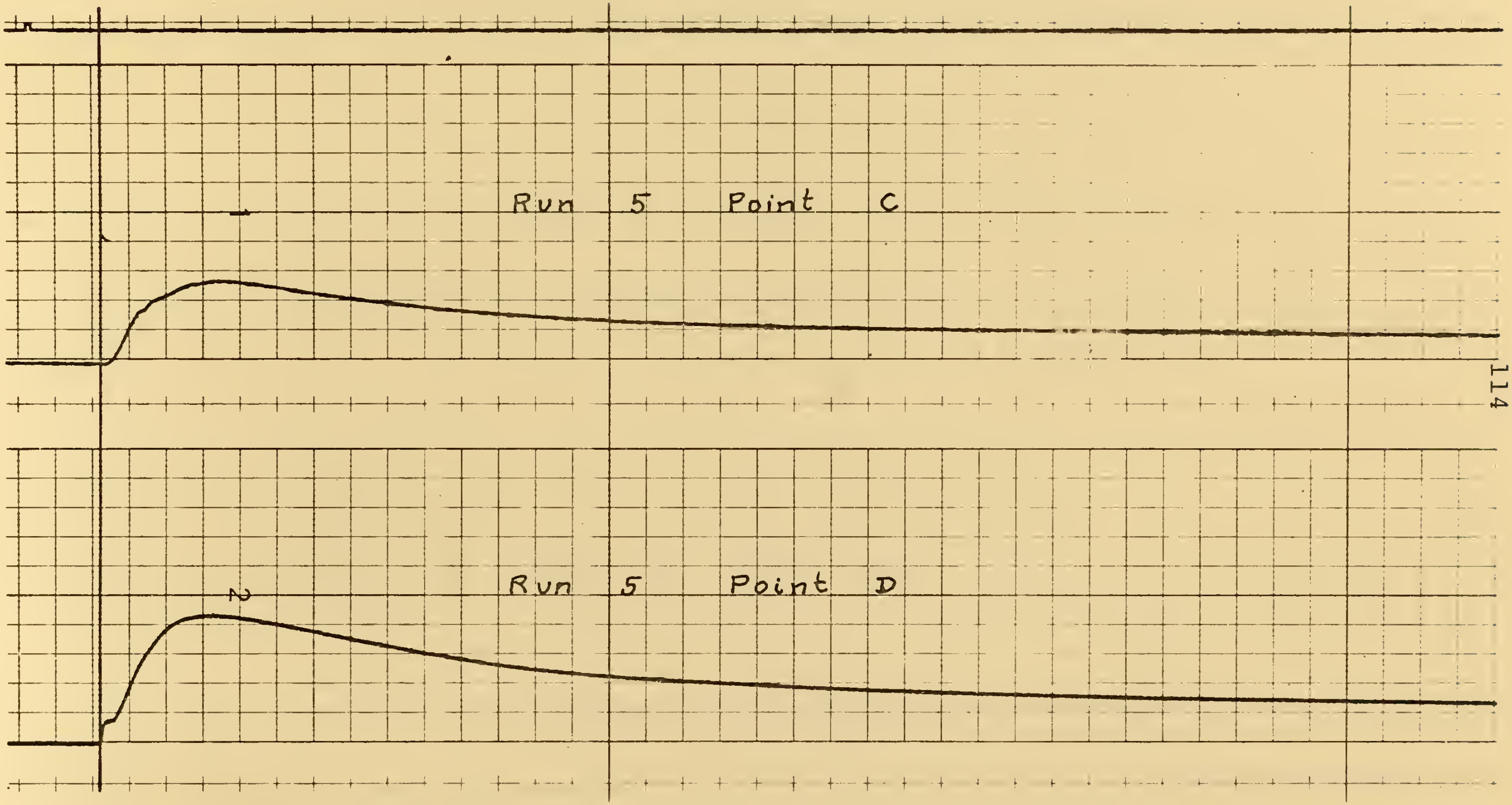
Run 5 Point C
1
2
Run 5 Point D

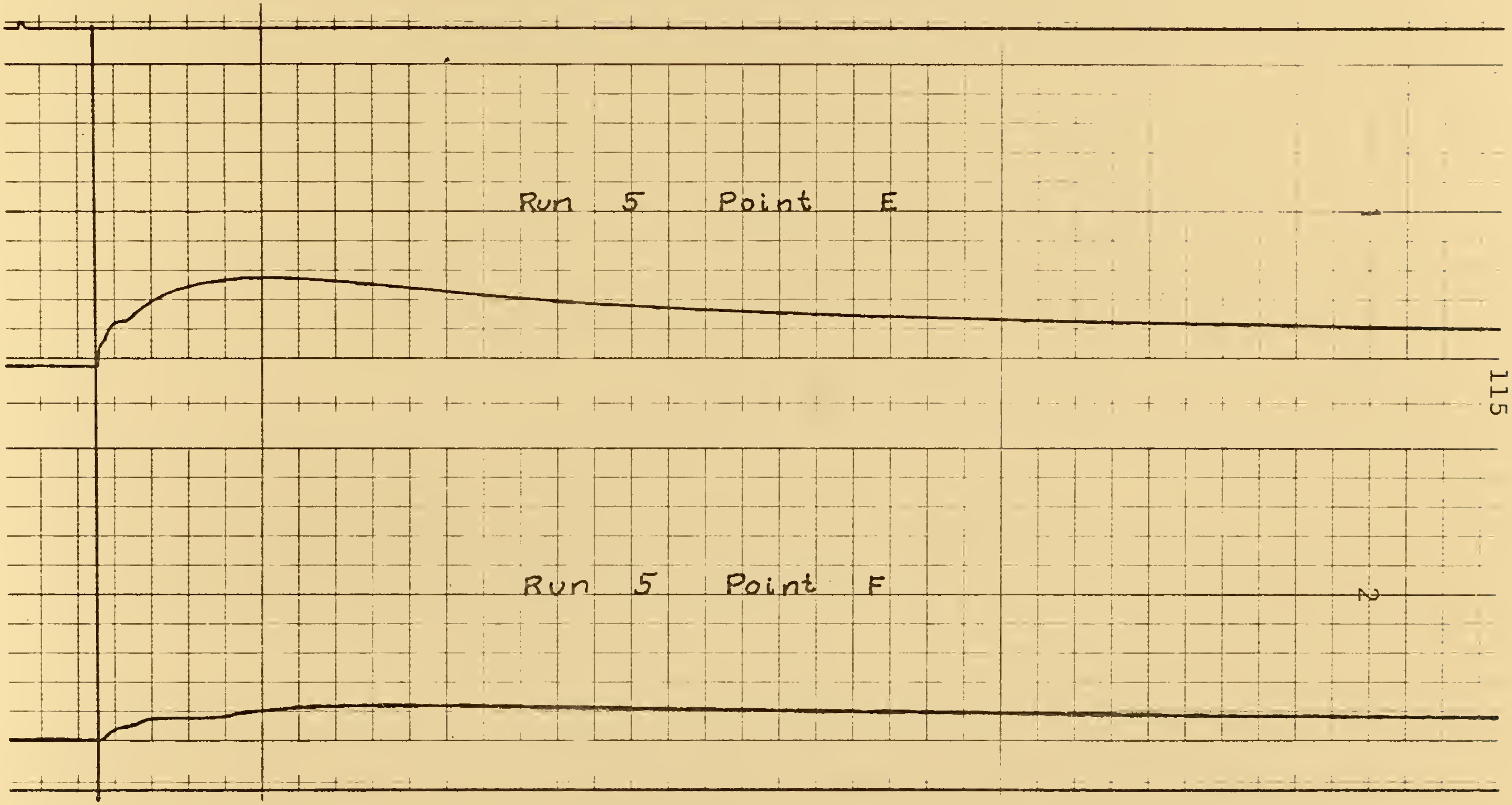
Run 5 Point E
1
Run 5 Point F
2